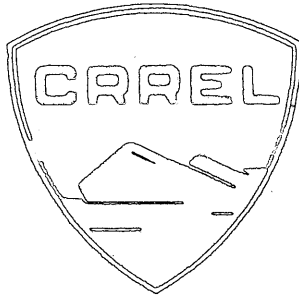


III-B1b



COLD REGIONS
SCIENCE AND ENGINEERING
Monograph III-B1b

ICE ENG. FAC.
DO NOT REMOVE
ICE PRESSURE
ON ENGINEERING STRUCTURES

Bernard Michel

June 1970

CORPS OF ENGINEERS, U.S. ARMY
COLD REGIONS RESEARCH AND ENGINEERING LABORATORY
HANOVER, NEW HAMPSHIRE

THIS DOCUMENT HAS BEEN APPROVED FOR PUBLIC RELEASE
AND SALE; ITS DISTRIBUTION IS UNLIMITED.

ICE PRESSURE ON ENGINEERING STRUCTURES

Bernard Michel

June 1970

DA PROJECT 1T062112A130

CORPS OF ENGINEERS, U.S. ARMY
COLD REGIONS RESEARCH AND ENGINEERING LABORATORY
HANOVER, NEW HAMPSHIRE

THIS DOCUMENT HAS BEEN APPROVED FOR PUBLIC RELEASE
AND SALE; ITS DISTRIBUTION IS UNLIMITED.

PREFACE

This monograph was prepared by Dr. Bernard Michel, Professor of Civil Engineering, Laval University, Quebec, P.Q., Canada, under contract with the U.S. Army Cold Regions Research and Engineering Laboratory (USA CRREL). It is published under DA Project 1T062112A13001, *Cold Regions Research - Applied Research and Engineering*.

CONTENTS

	Page
Preface	ii
Plan of the series of monographs on cold regions science and engineering	vi
Forces exerted by an expanding ice sheet	1
Introduction	1
Basic meteorological data	2
Temperature fluctuation inside the ice cover	3
Plastic behavior of ice submitted to increasing temperatures	7
Computation of ice thrust	10
Secondary factors	13
Static pressure against isolated structures	14
Protection against static ice pressure	14
Shore effects in thermal expansion of lake ice	16
Impact forces of ice on structures	18
Introduction	18
Strength of ice under impact loading	19
Indentation of ice by a pier with vertical edge	22
Splitting of ice floes by a pier with a vertical edge	27
Failure of ice floes on inclined piers	29
Verification and utilization of method	34
Miscellaneous effects of moving ice	35
Vertical forces exerted by ice on hydraulic structures	38
Introduction	38
Lifting force on isolated structures	39
Vertical force on a straight wall	43
Strength of adhesion of ice to structures	44
Icebreakers	44
Introduction	44
The mechanics of icebreaking	46
Characteristics of icebreakers	55
Ice models	58
Introduction	58
Laws of complete similitude	58
Practical limitations to ice modeling	63
Models representing only the hydrodynamic behavior of ice	63
Models for studying the collapse of an ice sheet	65
Future of ice modeling	67
Literature cited	67

ILLUSTRATIONS

Figure	
1. Mean coefficient of linear thermal expansion of ice	2
2. Effect of a snow cover on the temperature at a depth of 6 in. inside an ice cover	4

CONTENTS (Cont'd)

ILLUSTRATIONS (Cont'd)

Figure	Page
3. Computed and measured values of the ice temperature at a depth of 6 in. in the cover	6
4. Ice temperatures and pressures with time	8
5. Average pressure-time curves for temperature rises of 2°, 5°, 10° and 15° F/hr	8
6. Curve of percent of maximum pressure and percent of time to reach it	9
7. Curves of maximum pressure and initial temperature on a base of rate of temperature rise	9
8. Curves of time to reach maximum pressure and initial temperature on a base of rate of temperature rise	9
9. Relationships among creep parameters for granular-grained ice	9
10. Measured pressure distribution in a cross section of an ice sheet	11
11. Thrust of an ice sheet and rate of rise of air temperature	11
12. Maximum thrust exerted by an expanding ice sheet for various ice thicknesses at three latitudes and three initial air temperatures	12
13. Reduction in reservoir water level to compensate for ice thrust	15
14. Ice ramparts	16
15. Movement of ice on the shore of Wamplers Lake, Michigan	17
16. Orthogonal cracks on Wamplers Lake, Michigan	17
17. Steel stop-log, 88 ft long, broken by ice impact	18
18. Crushing strength vs temperature of ice on Portage Lake, Michigan	20
19. Influence of strain rate on the crushing strength of laboratory-made columnar ice with horizontal c-axes	21
20. Crushing of an ice floe on a pier	23
21. Indentation test	24
22. Stress zones in an indented block of ice	24
23. Splitting of an ice floe by a pier having a vertical edge	28
24. Failure of ice on the inclined edge of a pier	30
25. Progressive bending failures of an ice sheet at an inclined edge of a pier ...	32
26. Round edge and equivalent angle of a sharp-edged pier	33
27. Ice boom deflecting ice	36
28. Accumulation of ice on the shore of Lake Erie	37
29. Horizontal pressure of ice accumulation against a vertical wall	37
30. Infinite plate under load	41
31. Elastic and plastic failures of a radially cracked ice sheet	41
32. Variables and nomenclature used in ramming analysis	49
33. Ice resistance in pack ice of <i>Lena</i>	54
34. Ice resistance in pack ice for the <i>Stalin</i> and <i>Kapitan Belousov</i>	54
35. The <i>John A. MacDonald</i> breaking a jam at the Quebec bridge over the St. Lawrence River	57
36. Lines and particulars of U.S.S. <i>Glacier</i>	57
37. Coefficient of resistance in ice for scale models of icebreaker <i>Lenin</i>	64
38. Water level and discharge for model and prototype	65
39. Model of an ice-retaining boom, Laval University	65

CONTENTS (Cont'd)

TABLES

Table	Page
I. Maximum rate of linear air temperature rise in °F/hr for various time intervals	3
II. Total thrust exerted by expanding ice sheet	13
III. Range of ice strength as measured	19
IV. Design values of ice strength for impact loading	21
V. Values of contact coefficient ζ according to Korzhavin	25
VI. Shape factor, n , and pier angle, $2a$	29
VII. Values of coefficient C_0	33
VIII. Measured and calculated ice thrust	34
IX. Adhesion of ice to various materials and coatings	45
X. Icebreakers without fore propellers	56

PLAN OF THE SERIES OF MONOGRAPHS ON COLD REGIONS SCIENCE AND ENGINEERING

by

F.J. Sanger

The series consists of monographs written by specialists to summarize existing knowledge and provide selected references on the cold regions, defined here as those areas of the earth where operational difficulties caused by freezing temperatures may occur.

Sections of the work are being published as they become ready, not necessarily in numerical order but fitting into this plan, which may be amended as the work proceeds:

I. Environment

- A. General – Characteristics of the cold regions
 - 1. Selected aspects of geology and physiography of the cold regions
 - 2. Permafrost (Perennially frozen ground)
 - 3. Climatology
 - a. Climatology of the cold regions: Introduction, Northern Hemisphere I
 - b. Climatology of the cold regions: Northern Hemisphere II
 - c. Climatology of the cold regions: Southern Hemisphere
 - d. Radioactive fallout in northern regions
 - 4. Vegetation
 - a. Patterns of vegetation in cold regions
 - b. Regional descriptions of vegetation in cold regions
 - c. Utilization of vegetation in cold regions
- B. Regional
 - 1. The Antarctic ice sheet
 - 2. The Greenland ice sheet

II. Physical Science

- A. Geophysics
 - 1. Heat exchange at the ground surface
 - 2. Exploration geophysics in cold regions
 - a. Seismic exploration in cold regions
 - b. Electrical, magnetic and gravimetric exploration in cold regions
- B. Physics and mechanics of snow as a material
- C. Physics and mechanics of ice
 - 1. Snow and ice on the earth's surface
 - 2. Ice as a material
 - a. Physics of ice as a material
 - b. Mechanics of ice as a material
 - 3. The mechanical properties of sea ice
 - 4. Mechanics of a floating ice sheet
- D. Physics and mechanics of frozen ground
 - 1. The freezing process and mechanics of frozen ground
 - 2. The physics of water and ice in soil

III. Engineering

- A. Snow engineering**
 - 1. Engineering properties of snow
 - 2. Construction
 - a. Methods of building on permanent snowfields
 - b. Investigation and exploitation of snowfield sites
 - c. Foundations and subsurface structures in snow
 - d. Utilities on permanent snowfields
 - e. Snow roads and runways
 - 3. Technology
 - a. Explosions and snow
 - b. Snow removal and ice control
 - c. Blowing snow
 - d. Avalanches
 - 4. Oversnow transport
- B. Ice engineering**
 - 1. River-ice engineering
 - a. Winter regime of rivers and lakes
 - b. Ice pressure on structures
 - 2. Drilling and excavation in ice
 - 3. Roads and runways on ice
- C. Frozen ground engineering**
 - 1. Site exploration and excavation in frozen ground
 - 2. Buildings on frozen ground
 - 3. Roads, railroads and airfields in cold regions
 - 4. Foundations of structures in cold regions
 - 5. Sanitary engineering
 - a. Water supply in cold regions
 - b. Sewerage, and sewage disposal in cold regions
 - c. Management of solid wastes in cold regions
 - 6. Artificial ground-freezing for construction
- D. General**
 - 1. Cold-weather construction
 - 2. Materials at low temperatures
 - 3. Icings

IV. Remote Sensing

- A. Systems of remote sensing**
- B. Techniques of image analysis in remote sensing**
- C. Application of remote sensing to cold regions**

ICE PRESSURE ON ENGINEERING STRUCTURES

by

Bernard Michel

FORCES EXERTED BY AN EXPANDING ICE SHEET

Introduction

One of the most important forces in the design of a dam in northern regions is the horizontal thrust applied to the structure by a solid sheet of ice. Although much progress has been made in estimating this force, there is still a long way to go before we get an accurate design value for it, mainly because of the inadequate basic knowledge of the deformation behavior of ice.

With time, the analysis of this problem has been more and more refined and design values of this pressure have been successively lowered. At the beginning of the century, for instance, many dams were designed for the condition of crushing ice,^{5*} which led to a value as high as 50 kips per linear foot.^{6*} At present, some plastic properties of ice are being taken into account, and values used by Canadian engineers vary between 10 and 15 kips/ft for rigid structures. For more flexible structures, like sluice gates, values in the vicinity of 5 kips/ft are more commonly used.¹⁹

The importance of a proper allowance for ice thrust is apparent when it is appreciated that for a dam 38 ft high, an ice thrust of 15 kips/ft has the same tendency to tip the dam as the water pressure it was designed to resist.

There have been few reported dam failures caused by ice pressure^{22 23} and some engineers have doubted the advisability of making substantial allowances for this pressure in the design of hydraulic structures. But measurements made during the last few years leave no doubt as to its importance. A maximum recorded pressure of 3.5 kips/ft was measured on a tainter gate of the Hasting Dam³⁴ on the Mississippi River during the winter of 1932-33. A panel instrumented⁷² and set flush with the face of Des Joachims Dam during the winter of 1951-52 showed a maximum pressure of 6.9 kips/ft. Extensive measurements were made from 1946 to 1951⁴⁸ at several reservoirs in the mountains of Colorado. Indenter and strain gauges were set in thin mortar panels that could be installed on the face of the walls and at sites exposed to ice thrust. The maximum measured ice pressure at Eleven Mile Canyon was 16 kips/ft in 1947-48, 14 kips/ft in 1948-49 and 20 kips/ft in 1949-50. In the winter of 1950-51 tests were made at a number of reservoirs presenting a variety of shore conditions. At Antero and Shadow Mountains, where reservoirs have flat shores, maximum thrusts of 3.6 and 5.8 kips/ft, respectively, were measured. At the Evergreen reservoir, with moderately steep shores, the greatest thrust attained 9.4 kips/ft. The highest thrust of all, 17 kips/ft, was recorded at Tarryall Reservoir which has steep rocky shores in the vicinity of the dam. Similar tests were carried out by VNIIG⁴⁰ from 1954-56 in the Ges Reservoir of the Dnieper River. Maximum recorded ice pressure was 8.3 kips/ft.

The importance of ice thrust in the economic design of hydraulic structures requires it to be evaluated as accurately as possible at each site. Its value depends greatly on meteorological

*Superscript numbers refer to literature listed on page 67.

conditions and on the restraint caused by the topography of the reservoir shores. It is a rule of thumb²⁵ that this force can be ignored in regions where the mean January air temperature is above 40°F (4½°C).

Basic meteorological data

Rising air temperature, with or without absorption of solar radiation, causes an ice sheet to expand. The coefficient of linear expansion of ice⁸ is close to $28 \times 10^{-6}/^{\circ}\text{F}$ as shown on Figure 1, so that if an ice sheet 1 mile long were free to expand it would lengthen 53 in. for a 30°F (17°C) temperature rise. Considerable forces have to be exerted by the shores of a water body or by a structure to prevent, and compensate for, this type of expansion.

It is not easy to analyze the air temperature variations occurring in nature at a given site and to choose the values that are liable to produce the maximum thrust for design purposes. In most cold regions the mean rise of air temperature rarely exceeds 5°F/hr (3°C/hr) for a long enough interval of time but cases have been known,⁴ mainly in the chinook belt,* where the temperature rose 40°F (22°C) in 40 minutes, the rise being followed by an equally rapid fall with no perceptible interval in between. Many such variations are reported in the literature but because of their very short duration they are not representative of the temperature fluctuation inside the ice sheet itself which has a great thermal inertia.

The best way to approach the meteorological data of air temperatures in a region, for the purpose of obtaining the maximum ice thrust, is to separate the temperature rises in classes with simple laws of rise as a function of time. Three types of simplified analytical laws are representative of temperature fluctuations: the step function where the temperature rises suddenly and stays for a while at the new value, the linear increase for a long enough interval of time, and finally the diurnal sinusoidal variation of the air temperature. For a given total temperature rise the first type of variation is the worst that can happen to provoke maximum thrust in an ice sheet. However, it cannot be found at many places in nature with sufficiently high values of the step function. The case of the linear rise of the air temperature is universal and can be found for extended intervals of

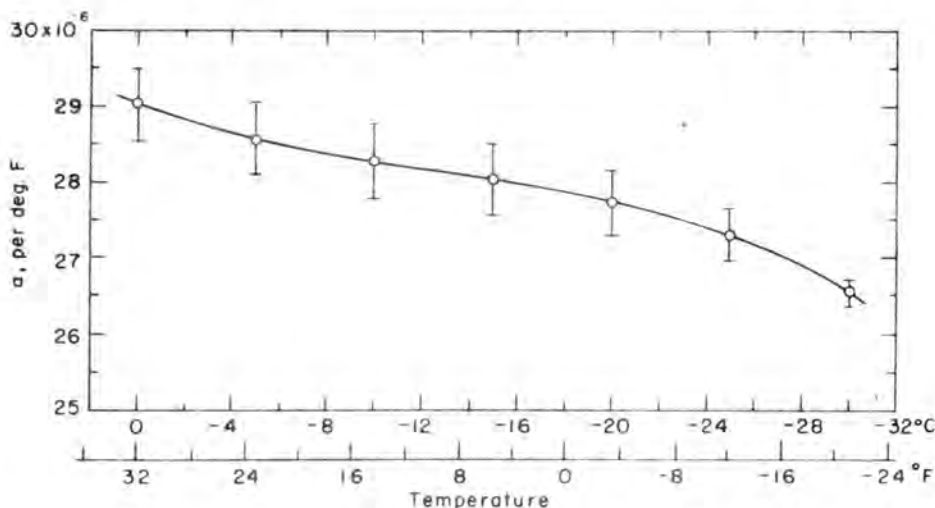


Figure 1. Mean coefficient of linear thermal expansion of ice. Standard deviations are shown.⁸

*A region where strong, warm, dry winds of short duration descend the eastern slopes of the Rocky Mountains.

time. For the same total air temperature fluctuation the temperature in the ice itself is much more damped with a sinusoidal variation than with a linear rise and only this latter law need normally be taken into account.²⁰

The analysis of the characteristics of the linear rise in air temperature to be used for design purposes must take into account two variables: the total temperature rise ΔT_m and the time interval Δt required to obtain that rise. For each interval of time Δt from let us say 5 hours to 20 hours it is possible to find the greatest rise in air temperature every year for the period of observations at the site. A typical statistical analysis of these data²⁰ for 23 winters at Quebec City (Table I) will then determine the maximum possible rise and its duration for any expected period of return. It is interesting to note, for the case previously cited, that there was an upper limit to the rate of temperature rise (7°F/hr ; 4°C/hr).

This case is not general, however, and a predetermined period of return must be chosen to obtain design values. The return period must then be based on an economic valuation criterion to minimize the added cost of construction and the cost of the risk of damage.⁶ This may essentially lead to short periods of return of the expected event, of the order of 20 years.

Table I. Maximum rate of linear air temperature rise in $^\circ\text{F/hr}$ for various time intervals (Quebec City, Canada).

Period of return (years)	Time intervals in hours							
	5	6	7	8	9	10	15	20
12.5	4.4	4.2	4.3	3.9	3.5	3.1	2.1	1.6
25	4.7	4.5	4.7	4.1	3.7	3.3	2.2	1.7
50	5.2	5.0	5.0	4.4	3.9	3.5	2.3	1.8
100	5.6	5.3	5.3	4.6	4.1	3.7	2.5	1.9
200	6.0	5.7	5.6	4.9	4.3	3.9	2.6	2.0
500	6.6	6.2	5.8	5.1	4.7	4.1	2.7	2.1
1000	7.0	6.5	6.1	5.4	4.8	4.3	2.9	2.2

Temperature fluctuation inside the ice cover

Many factors influence the temperature distribution inside an ice cover for a given air temperature fluctuation. There is first a difference between the temperature at the ice surface and the temperature of the air because of the thermal boundary layer in the air. But the difference is small and measurements made for a whole winter²⁰ on clear ice have shown that it rarely exceeds 3°F (1.7°C). It is thus safe and acceptable to neglect this effect.

The thermal conductivity of freshly fallen snow is from 10 to 30 times less than that of ice. A few inches of snow on an ice cover acts as a practically perfect insulator and no sensible temperature fluctuation is transmitted to the ice sheet. Figure 2 shows the dramatic effect of 9 in. of snow on the temperature at a depth of 6 in. in a 12-in. ice cover at Eleven Mile Reservoir, Colorado.⁴⁹ This is one of the reasons why young and relatively thin ice exerts the highest pressure on a dam at the beginning of winter. Little allowance for ice pressure need be made during the period that a snow cover is expected to stay on the ice. It must also be borne in mind that a uniform fresh snow cover will also, by its weight, drown an ice cover of approximately the same thickness, so that the mechanism of heat transfer is completely modified. At least, no thrust is developed while the ice sheet is forming again at the top.

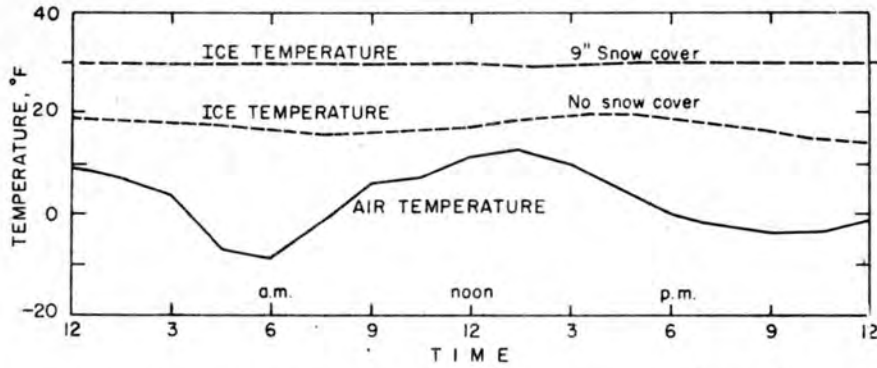


Figure 2. Effect of a snow cover on the temperature at a depth of 6 in. inside an ice cover.⁴⁹

The temperature distribution inside an ice cover can be obtained from the Fourier equation:

$$\frac{\partial T}{\partial t} = H_i^2 \frac{\partial^2 T}{\partial x^2} \quad (1)$$

where:

T = temperature of the ice, °F

t = time, hours

x = distance of a point from the lower ice surface, ft

H_i^2 = coefficient of diffusivity of ice, which can be taken as 0.0434 ft²/hr.¹⁸

The equation can be solved for the simpler boundary conditions discussed previously.⁶⁶ The simplest case is that of determining the temperature changes (ΔT) in an ice sheet originally at a steady state when it is exposed to surroundings below freezing temperature. The computation then gives:

$$\Delta T = \frac{K_c \left(\frac{h}{K} \right)}{1 + K_c \left(\frac{h}{K} \right)} T_1 \left\{ \left[\sum_{n=1}^{\infty} A_n \exp - \frac{H_i^2 \alpha_n^2}{h^2} t \sin \frac{\alpha_n x}{h} \right] + \frac{x}{h} \right\} \quad (2)$$

where:

$$A_n = \frac{-2 (\sin \alpha_n - \alpha_n \cos \alpha_n)}{\alpha_n (\alpha_n - \sin \alpha_n \cos \alpha_n)}$$

and the α_n are the successive positive roots of the equation:

$$\tan \alpha = \frac{K \alpha}{K_c h}$$

Here K is the thermal conductivity of ice, h the total thickness of the ice sheet, T_1 the value of the air temperature rise and K_c the film conductance of convection in Btu/ft² hr^oF.

The second case is that of a linear temperature rise at a rate \dot{T}_0 . It then gives:

$$\Delta T = \frac{K_c \left(\frac{h}{K}\right)}{1 + K_c \left(\frac{h}{K}\right)} \dot{T}_0 \left\{ \left[\sum_{n=1}^{\infty} A_n \frac{h^2}{H_i^2 \alpha_n^2} \left(1 - \exp - \frac{H_i^2 \alpha_n^2}{h^2} t \right) \sin \frac{\alpha_n x}{h} \right] + \frac{x}{h} t \right\}. \quad (3)$$

Another important factor affecting the rise of temperature inside an ice cover is the absorption of solar energy. This effect can be introduced in the computation. If we consider only the absorbed heat of solar radiation at the surface of the ice sheet ψ_r in Btu/ft² hr, we then obtain:

$$\Delta T = \frac{\psi_r(t)h}{1 + \left(K_c + K_r\right)\frac{h}{K}} \left\{ \left[\sum_{n=1}^{\infty} A_n \exp - \frac{H_i^2 \alpha_n^2}{h^2} t \sin \frac{\alpha_n x}{h} \right] + \frac{x}{h} \right\} \quad (4)$$

where K_r is the film conductance of radiation in Btu/ft² hr^oF.

For the case of temperature change due to absorption within the ice sheet of part of that portion of the solar energy transmitted through the ice, an additional term is required in the heat equation which becomes:

$$\frac{\partial T}{\partial t} = H_i^2 \frac{\partial^2 T}{\partial x^2} + \dot{T}_r(t) \exp - \psi_r' h \left(1 - \frac{x}{h} \right) \quad (5)$$

where ψ_r' is the absorptivity of ice and \dot{T}_r is the solar volume absorption coefficient of ice at the surface (i.e. temperature change per unit time).

The solution of this equation for the proper boundary conditions is:

$$\Delta T = \left\{ \left[\sum_{n=1}^{\infty} B_n \exp - \frac{H_i^2 \alpha_n^2}{h^2} t \sin \frac{\alpha_n x}{h} \right] + C \left(1 - \exp \psi_r' x \right) + D \frac{x}{h} \right\} \quad (6)$$

where:

$$B_n = \frac{\frac{2 \exp - \psi_r' h}{(\psi_r' h)^2} \left\{ \alpha_n (1 - \cos \alpha_n) - \frac{\alpha_n^2}{\alpha_n^2 + (\psi_r' h)^2} \left[\exp \psi_r' h (\psi_r' h \sin \alpha_n - \alpha_n \cos \alpha_n) + \alpha_n \right] \right\}}{(\alpha_n - \sin \alpha_n \cos \alpha_n)} +$$

$$+ \frac{\frac{2}{\psi_r' h} + \frac{2}{(\psi_r' h)^2} (K_r + K_c) \frac{h}{T_0} (1 - \exp - \psi_r' h) (\sin \alpha_n - \alpha_n \cos \alpha_n)}{1 + (K_r + K_c) \frac{h}{K} (\alpha_n - \sin \alpha_n \cos \alpha_n)}$$

$$C = \frac{\dot{T}_r(t) \exp - \psi_r' h}{H_i^2 (\psi_r')^2}$$

$$D = \frac{\frac{\dot{T}_r(t) h}{H_i^2 \psi_r'} + \frac{\dot{T}_r(t)}{H_i^2 (\psi_r')^2} \frac{(K_c + K_r) h}{K} (1 - \exp - \psi_r' h)}{1 + (K_c + K_r) \frac{h}{K}}$$

By means of the above equations it is possible to compute the change in temperature of an ice sheet for a step or linear function of temperature rise and for absorption of solar radiation. The heat equation being linear, the temperature rise at any point can be obtained by adding up the effects of separate components. This was done⁴⁹ for a 40°F (22°C) temperature rise that occurred in 1 hour and 15 minutes in January 1947 at Eleven Mile Reservoir. The results are shown in Figure 3. The ice temperature is that of ice free of snow at a depth of 6 in. in an ice sheet 15 in. thick. The computed values are shown by the individual points near the smooth observed ice-temperature curve. The computed and measured values agree well.

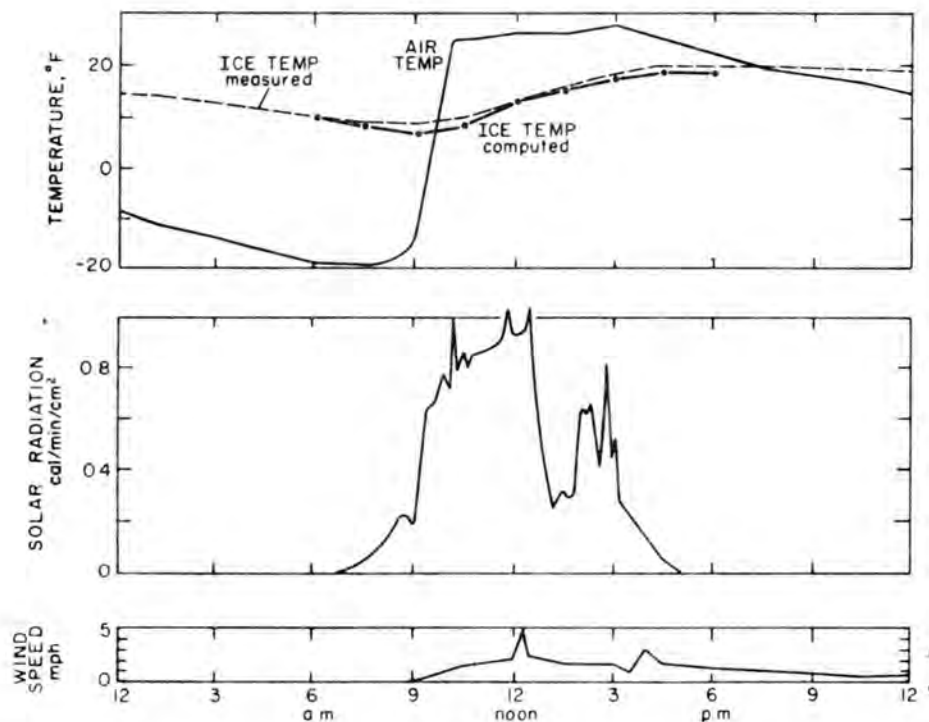


Figure 3. Computed and measured values of the ice temperature at a depth of 6 in. in the cover.⁴⁹

Plastic behavior of ice submitted to increasing temperatures

The most direct way of studying the behavior of ice under increasing temperature is to measure the force needed to keep a test sample at constant length between the loading blocks of a testing machine.

The latest measurements are those of Monfore⁴⁸ which were carried out on cylinders 4 in. in diameter and 4 in. long taken from lake ice, with the axes of the cylinders parallel to the surface of the ice sheet. Loads applied to the cylinders were thus in the same direction, relative to the crystal structure, as thrusts which develop in an ice sheet in the field.

Unfortunately Monfore made no study of the crystallographic structure of this ice. Many different types of ice can coexist in the same lake and their creep properties vary over a wide range of values for the same loading conditions. It is thus now impossible to ascertain if the values he obtained are representative of the ice types that will give the highest loading conditions in nature.

In these tests, ice temperatures were controlled by passing air through the test chamber and were measured inside the ice with copper-constantan thermocouples.

The ice in the testing machine was first brought to the desired initial temperature and was then held at this value until equilibrium was established. In order to obtain a given linear rate of temperature rise in the ice, it was necessary for the air temperature to rise at a much greater rate for about the first 15 minutes. As the temperature of the ice increased, the load on the sample was adjusted to maintain the ice at its initial length. Temperatures were read and the load on the sample was adjusted every 5 minutes for the first 30 minutes of test. Temperatures were read every 15 minutes and the load adjusted twice every 15 minutes thereafter.

The specimen length was kept constant with the help of a gauge set between each of the loading blocks. The loads to equilibrate the zero deformation were applied with a small hydraulic ram. The ram was operated by a hand pump equipped with a large pressure gauge calibrated directly in total load.*

More than 100 tests were carried out, and for each one of them the pressure rose to a maximum and then decreased. Ice temperatures and pressures for a typical test are shown in Figure 4. In this test the ice temperature rose from -10.5°F (-23.6°C) at a uniform rate of 5°F/hr (2.8°C/hr).

Check tests were run on several samples to determine the degree of reproducibility of apparatus and techniques. The average deviation in maximum pressures for duplicate tests on a given sample was 6.0%, which was considered satisfactory. Much larger variations, averaging 25%, were found in the maximum pressures reached by different ice samples tested under the same conditions. This seems to depend on the arrangement of crystals in apparently similar samples and it was eventually found that the samples that reached low maximum pressures contained crystal surfaces or other sharp divisions along which slippage might have occurred.

Pressure tests were made with initial temperatures of -30° , -10° and $+10^{\circ}\text{F}$ (-34.4° , -23.3° and -12.2°C) and with rates of temperature rise in the ice of 2° , 5° , 10° and 15°F/hr (1.1° , 2.8° , 5.6° and 8.3°C/hr). Curves similar to those of Figure 4 were obtained for each test. For a given rate of temperature rise, the maximum pressure reached by the sample increased as the initial temperature decreased; for a given initial temperature the maximum pressure increased as the rate of temperature rise increased. The relationships between the pressures and time for various initial temperatures and rate of temperature rise are shown in Figure 5.

All these results have basically the same form if they are compared on a non-dimensional basis as shown in Figure 6. The only two characteristic parameters are the maximum pressure and the time required to obtain this pressure (Fig. 7, 8).

*The use of this procedure of discontinuous load application to obtain the creep behavior of ice is very much open to question.

ICE PRESSURE ON ENGINEERING STRUCTURES

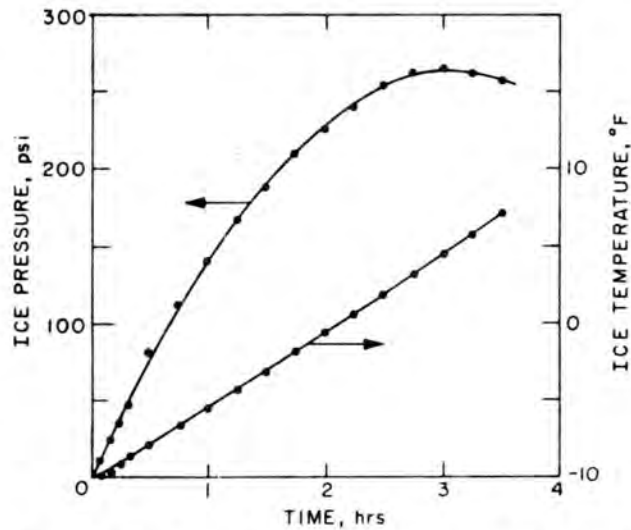


Figure 4. Ice temperatures and pressures with time.⁴⁸

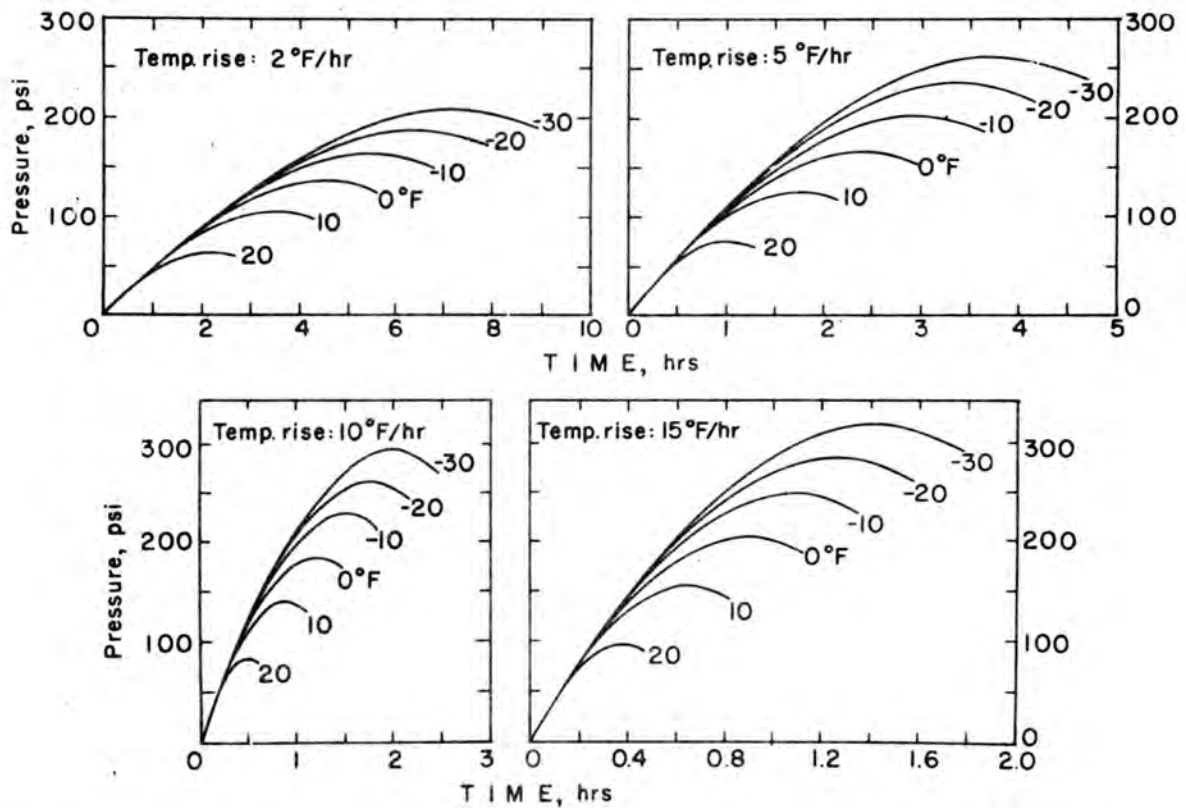


Figure 5. Average pressure-time curves for a temperature rise of 2° , 5° , 10° and 15°F/hr (1.1° , 2.8° , 5.6° and 8.3°C/hr) from indicated initial temperatures.⁴⁸

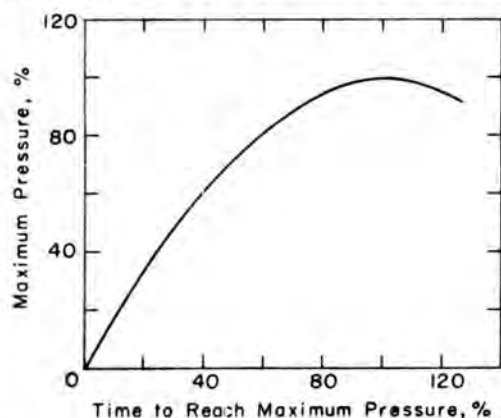


Figure 6. Curve of percent of maximum pressure and percent of time to reach it.⁴⁸

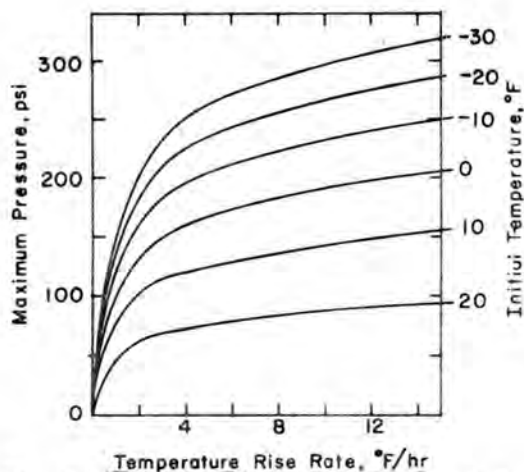


Figure 7. Curves of maximum pressure and initial temperature on a base of rate of temperature rise.⁴⁸

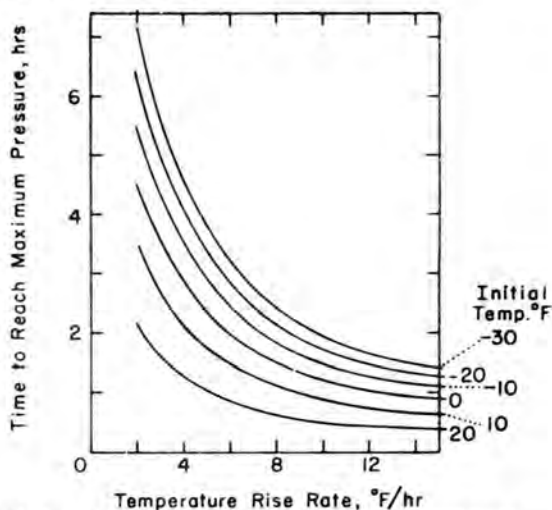
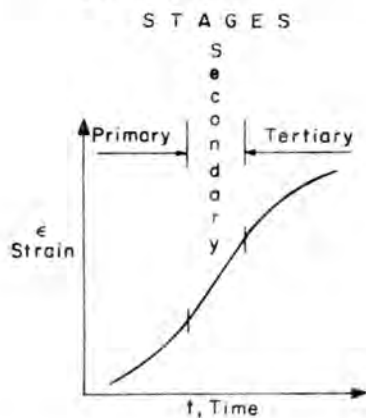
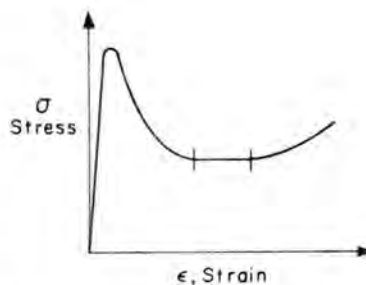


Figure 8. Curves of time to reach maximum pressure and initial temperature on a base of rate of temperature rise.⁴⁸



a. Creep at constant stress.



b. Stress at constant rate of strain.

Figure 9. Relationships among creep parameters for granular-grained ice.⁴¹

In a broad sense these results could be interpreted with the present knowledge of the basic behavior of granular-grained ice under creep loading conditions for compression stresses over approximately 140 psi. The deformation of this ice as a function of time can be represented⁴¹ by curves of the type in Figure 9a. In principle there are essentially three phases of ice deformation. At the beginning of the application of a constant load, there is a primary viscoelastic deformation. This is followed by secondary deformation at practically constant rate, the ice then behaving as a viscous substance. In the final (tertiary) stage, accelerated creep develops up to the failure of the ice sample.

It is also most interesting to observe this behavior under a second mode of loading. For a constant rate of deformation, the corresponding pressure curve is of the form shown in Figure 9b. During viscoelastic deformation, the pressure rises until it attains a maximum. It then decreases and stays constant during the secondary phase of deformation of the ice.

There is little doubt that this basic ice behavior is representative of the behavior of an ice sheet submitted to thermal stresses that produce significant ice thrusts, as Figure 6 shows. The main drawback of this explanation lies in the fact that the high stresses measured by Monfore have not been observed for uniaxial compression with the values of strain rates induced by thermal expansion. Two other factors have also to be taken into account in this interpretation: the effect of biaxial expansion and the influence of the temperature of the ice itself on its creep properties.

Computation of ice thrust

The distribution of stresses as a function of time inside an ice cover subjected to a linear temperature rise can be represented⁴³ with the typical measurements shown on Figure 10. It can be seen that after the maximum stress is attained at the surface of the ice sheet the stress starts to decrease at this point while it continues to increase underneath. Thus, a few measurements show generally that the total maximum thrust occurs slightly after the maximum stress is attained at the upper surface and its value may be from 10 to 20% higher.

Because so little is known of creep properties of ice and because appreciable differences in creep rates may exist between different kinds of ice under different loading conditions, even for very small changes in internal structure, the analysis was limited here to the computation of the thrust developed when the maximum stress was attained at the upper surface for Monfore's ice. At the present time this is all that can be used as an indication for design purposes and it is expected to give values very much on the high side.

The total thrust was computed with the usual assumptions for this problem:⁶⁰

1. The initial air temperature is -30°F , -10°F and 10°F (-34.4° , -23.3° and -12.2°C).
2. The initial ice temperature varies linearly from -30°F (-34.4°C) at the upper surface to $+32^{\circ}\text{F}$ (0°C) at the lower surface.
3. The air temperature changes at rates of 2° to 15°F/hr (1.1° to 8.3°C/hr).
4. The temperature of the ice at the surface is assumed to be the same as the air temperature.
5. The thickness of the ice sheet remains constant.

The temperature distribution and the rate of temperature rise inside the ice sheet were computed²⁰ by eq 3 for variable ice sheet thicknesses, air temperature rises and initial ice temperatures.

Figure 11 shows that for an ice sheet of given thickness the maximum thrust is attained for an air temperature rise of only 3°F/hr (1.7°C/hr). This can be explained by the fact that at this rate

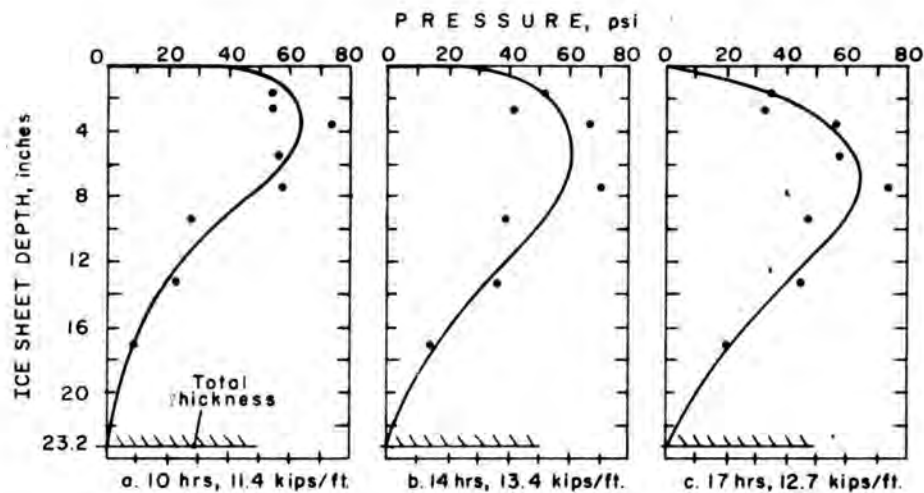


Figure 10. Measured pressure distribution in a cross section of an ice sheet.⁴³

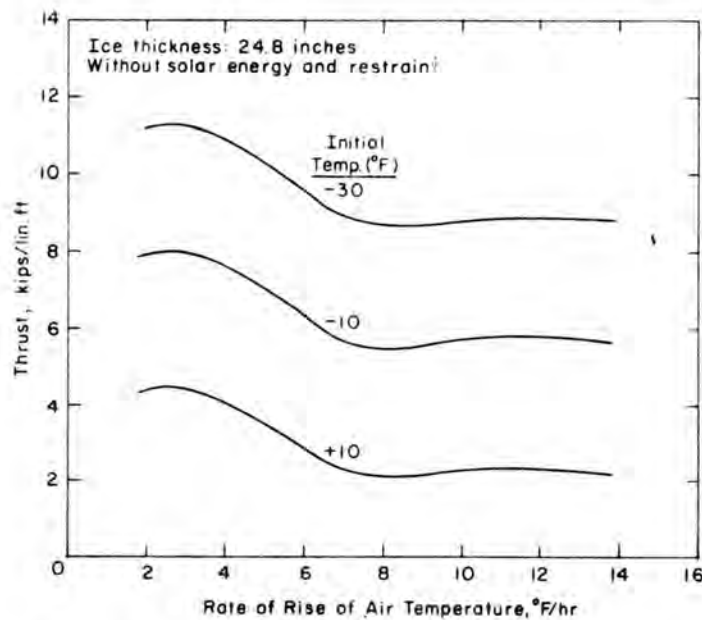


Figure 11. Thrust of an ice sheet and rate of rise of air temperature.²⁰

there is enough time for the ice to develop an important overall thrust before the maximum pressure is attained at the surface when the computation is stopped. The curves also show an inflection point at a rate of about 7.6°F/hr (4.2°C/hr). This can be explained from the rheological behavior of Monfore's ice in this area (Fig. 7) where there is a sharp change in the variation of the maximum pressure that this ice can exert.

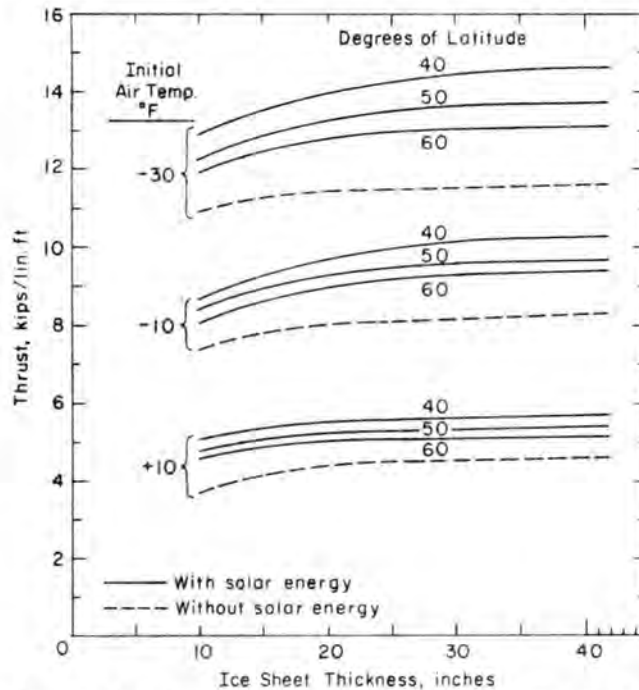


Figure 12. Maximum thrust exerted by an expanding ice sheet for various ice thicknesses at three latitudes and three initial air temperatures.²⁰

The effect of ice thickness is shown in Figure 12. The thrust does not increase appreciably for ice sheets thicker than 12 in., mainly because there is no sensible variation of temperature below this point before the stresses start to decrease at the upper surface. Furthermore, if we also consider that snow covers are related to thicker ice sheets, there is little doubt that the maximum thrust does not increase appreciably for ice sheets thicker than 12 in.

When the ice sheet is free of snow and exposed to sunlight, its temperature may have an added increment by absorption of solar radiation, quite apart from the change caused by an increase in air temperature.

The magnitudes of ice thrusts were computed to include solar energy effects with the following additional assumptions:²⁰

7. The latitudes are 40°, 50° and 60°.
8. The vernal equinox is the time limit for the formation of clear solid ice of adequate thickness.
9. The atmospheric transmission constant is 0.9, based on a clear atmosphere at a fairly high elevation.
10. The coefficient of heat transfer is 2 Btu/ft² hr °F, to allow for surface losses of the absorbed solar energy.

For these assumed conditions the solar energy that reaches the surface of the ice sheet during midday is about 250 Btu/ft² hr at 40° latitude, 200 Btu/ft² hr at 50° latitude and 150 Btu/ft² hr at 60° latitude. The absorptivity of ice is small in the visible spectrum¹⁴ but beyond a wavelength of 1 micron it is great and is analogous to that of water. Consequently, about 40% of the solar energy

reaching the surface, essentially all that of wavelength greater than 1 micron, is absorbed within 4 in. of the surface. For a clear ice sheet 1 ft thick an additional 15% of the energy is absorbed, whereas for a 4-ft thickness this additional absorption amounts to about 25%. Most of the remainder of the energy is transmitted although a small percentage is reflected.

The effect of solar energy was computed²⁰ using eq 4 and the results (Fig. 12) indicate that the absorption of this energy may produce a considerable increase in thrust above that caused by the rise of the air temperature.

The effect of lateral restraint was estimated on the basis of the behavior of an elastic slab. Elastic behavior is approached only for the conditions of very rapid strain rates when flow is small. Poisson's ratio ν may not be applicable for flow conditions, but pressures based on elastic behavior for restraint conditions might give the most severe loading conditions. The ratio of increase in stress for complete lateral restraint to the stress developed for no lateral restraint is given by $\nu/(1 - \nu)$. The values computed for no lateral restraint are increased by this factor and are shown in Table II.

Table II. Total thrust exerted by expanding ice sheet (Monfore's ice).

Ice thickness greater than 12 in., no solar energy.

Ice surface temp rise	Initial air temperature					
	-30°F		-10°F		$+10^{\circ}\text{F}$	
	Lateral restraint		Lateral restraint		Lateral restraint	
	No	Yes	No	Yes	No	Yes
3°F/hr	11.5	18	8.1	12.7	4.5	7.1
5°F/hr	10.6	16.6	7.3	11.3	3.5	5.5
10°F/hr	8.8	13.8	5.8	9.1	2.4	3.7
15°F/hr	8.6	13.4	5.6	8.9	2.2	3.5

Secondary factors

Observations on lakes free of snow⁶⁰ have shown that reefs and pressure ridges formed by the expansion and buckling of an ice sheet seldom occur when the ice is thicker than 1 ft, although they have been known to form in ice 20 in. thick. This phenomenon might be interpreted to indicate that for ice sheets less than 1 ft thick the critical buckling load is the limiting factor governing the ice pressure on a dam, whereas for thick ice sheets the pressure may develop to its maximum without buckling of the sheet. These observations have been somewhat correlated by a computation in the first approximation,⁴³ assuming very approximate plastic ice properties, where it is shown that buckling is a limiting factor when the ice thickness is less than 1.5 ft thick. For ice sheets 2 ft thick, which would normally be considered for design purposes, this limitation need not be taken into account.

When an ice sheet increases in thickness in a reservoir and the temperature falls, tensile stresses are set up in the ice, giving rise to contraction cracks. When the ice is heated up again the gap in the crack, if it has not already frozen, will first have to be taken up by the expanding ice before any thrust can be exerted. This phenomenon thus reduces the force exerted by an expanding ice sheet.

Many other factors tend to reduce the thrust of ice compared to the thrust that can be computed. An important one is the difference between the behavior of a small ice sample in a laboratory and

a large ice sheet in nature. Because of cracks, faults, internal dislocations and discontinuity in a large ice sheet a small sample is always stronger than the ice in the field. It has also been shown³¹ that the creep rate of ice increases under reloading conditions. An ice sheet submitted to cycles of contraction and expansion during its growth will exert much lower pressure than what would be expected from the behavior of a laboratory sample tested for the first time.

Static pressure against isolated structures

The pressure of an expanding ice sheet on the tip of a protruding spillway pier set in the ice is somewhat higher than the pressure per unit length multiplied by the width of the pier. A first approximation of this value can be obtained with an empirical formula:⁵⁶

$$F = p_{\max} \left(B_0 + \frac{B'}{3} \right) \quad (7)$$

where:

F = maximum horizontal force, lb

p_{\max} = static pressure per unit length obtained for this case, lb/ft

B_0 = width of the pier, ft

B' = span between piers, ft.

For the case of a bridge pier this force has to be taken into account only if it is not balanced by an equal and opposite force on the downstream side of the pier. Because, in a general way, the turbulence of the flow in the wake of a pier might prevent ice from forming close to it, it might be safer in most applications to consider this force on the upstream edge.

Furthermore, the lateral ice pressures on a bridge pier usually balance each other on both sides. There are many cases, however, in high-velocity flow, where a channel may stay open in the winter between two bridge piers. If an ice sheet then forms on the other side of these particular piers, full allowance has to be made for lateral pressure. Such a state of loading may greatly affect the stability of piers.

Protection against static ice pressure

At an existing dam, designed with no allowance for ice pressure, the following procedure may be used to protect against expanding ice. Generally, all dams are designed for the full reservoir condition with the water surface at or very near the top of the dam. It is possible to compensate for the effect of ice thrust by lowering the reservoir level during the season when ice pressure may exist, so that the total load at the critical section is not larger than for the full reservoir condition.

Figure 13⁶⁰ shows the required lowering of a reservoir to balance the effect of the indicated ice thrusts. The criterion used for evaluation in Figure 13a is the moment at the base, whereas Figure 13b shows results with horizontal shear as the governing factor. The moment effect governs (that is, yields larger reductions in the water level) for all heights greater than those at the maximum points of the curves in Figure 13a. The height above which the moment governs and below which shear governs is shown by the lines marked "moment-shear line." The base of a dam is usually the critical section, but the curves can be applied to any other elevation by considering the height above the elevation in question. The curves are applicable to a gravity-type dam.

The curves indicate that in the case of high dams the ice thrust is of relatively minor importance in its effects on forces at the base of the section, whereas for low dams it is of considerable

Shore effects in thermal expansion of lake ice

Expansion and contraction of lake ice due to temperature changes has long been known to be responsible for the formation of ice ramparts along the shore areas, or of pressure ridges in the ice itself.

The underlying principle involved in the formation of ice ramparts has been well established.⁵ A rapid fall in air temperature causes the ice on a lake to contract, so that tension cracks are developed in the ice sheet. These cracks immediately fill with water, which quickly freezes, so that the total mass of the ice cover is increased. A subsequent rise in air temperature results in expansion of the ice, so that the total surface area is greater than it was before contraction. This increase in area of the ice cover results in compressive forces against the shore so that shore debris is forced into ridges called "ice ramparts" (Fig. 14).

Extensive measurements were made of this phenomenon at Wamplers Lake, Michigan, during the winters of 1951-52 and 1952-53.⁷³ The first winter a movement of ice on the shore of 1.6 ft was measured, of the type shown in Figure 15. The expansion movement of the ice was not normal to the shore but was related to the form of the lake; more expansion was observed along the long axis than along the short one on this oblique lake. In the second winter the lake level was lower and a new rampart was built at a lower level from boulders and gravel that were normally submerged beneath the water of the shore region.

On one occasion the atmospheric temperature dropped from 30° to 8°F (-1° to -13°C) in 12 hours and cracks developed with widths ranging from a few tenths of an inch to 1.5 in. The ice thickness at that time was 8 in. and the snow cover was 3½ in. One set of cracks radiated from the central part of the lake and another set roughly followed the shoreline. Figure 16 shows two of these orthogonal cracks.

It is interesting that the formation of a compression ridge was observed only once during these two winters, when the ice was 8 in. thick. The axis of this ridge lay at right angles to the direction of movement of the sheet as recorded by markers. Prior to this time no buckling had taken place, but considerable thrust had developed on the shore.



Figure 14. Ice ramparts.⁷³



Figure 15. Movement of ice on the shore of Wamplers Lake, Michigan.⁷³



Figure 16. Orthogonal cracks on Wamplers Lake, Michigan.⁷³

Finally it was observed that no appreciable movement of the markers occurred because of the skin friction caused by the wind.

IMPACT FORCES OF ICE ON STRUCTURES

Introduction

Most older river bridges of northern countries end their lives by pier movement following scour and ice pressure at breakup time. Very little has been written on this unfortunate event, although it would be quite revealing for the design of these structures. There is no doubt that one of the most important forces that can lead to the collapse of a bridge is the force of moving ice floes but only the failure of larger bridges under ice conditions has been, at times, reported in the literature. Examples are the Niagara Falls View bridge,⁵⁸ the Cushing bridge,⁵⁹ some Missouri highway bridges,³⁸ and the Brattleboro bridge.²¹

Ice may adversely affect a bridge in a number of ways. Premature snow melt in a river basin may suddenly increase the river flow, which in turn raises the solid ice sheet adhering to the piers, partially lifting them out and endangering the stability of their foundation. The piers may be located in such a manner in the river bed as to hinder the passage of ice, and to prime ice jams. These increase the pressure on the piers, and the superstructure may be destroyed if the ice is raised high enough to impinge on it. The water may also find a new channel within or around the ice jam and high-velocity flow may badly scour the approaches or the pier foundation. Finally the moving ice floes at breakup usually exert an appreciable force when hitting the bridge piers. This force may displace a pier enough to cause the collapse of the bridge.

Moving ice may also impinge on other types of hydraulic structures. Figure 17 shows a steel dam gate that failed under the impact of ice.



Figure 17. Steel stop-log, 88 ft long, broken by ice impact (1967).

In North America the practice has generally been to compute the impact force of ice on structures with the design code of the AASHO.¹ It simply says that one has to apply a horizontal component of force to the pier equal to the projection of the ice area perpendicular to the axis of the flow, multiplied by the crushing strength of ice, which is recommended to be taken as 400 psi. This computation usually leads to considerable ice forces that increase the cost of bridges. The code values are widely questioned by bridge designers because of the supposedly high value taken for the crushing strength of ice and mainly because they do not take into account any mode of failure other than compression although piers are designed specially to shear or lift the floes out of the water in order to reduce this force. We will now review the most important recent work on this question, principally that of Korzhavin.⁴⁰

Strength of ice under impact loading

Under conditions of quick loading as when an ice floe hits a bridge pier, ice behaves like a brittle material and its ultimate strength can be determined. Because ice is formed in nature under various conditions there is a wide spread in the results of tests made to determine its mechanical properties. This question is discussed extensively in the CRREL monographs on physics and mechanics of ice (see CRSE Monograph II-C2, *Ice as a material**) and we will discuss here the engineering properties of interest for this application.

We are concerned with river and lake ice which can usually be divided into clear lake ice and snow ice. The clear lake ice usually consists either of a fabric of prisms with their lengths normal to the ice sheet, or of congealed frazil slush. The columnal crystals usually increase in diameter with depth and the number of crystals at a given depth decreases accordingly. The crystal size varies, depending probably on the freezing conditions, from a fraction of an inch to several inches across. On the surface of the sheet there is usually a layer of ice, called snow-ice, made of small compact grains. In a lake this ice is formed either from a snowfall freezing into the water surface or when water sweeps through the ice cover, saturates the snow cover, and then freezes. The freezing of slush and frazil forms congealed frazil slush which is normally transparent ice of granular structure. Snow ice usually contains many air bubbles and is weaker than clear lake ice.

The mechanical properties of river and lake ice depend on a number of factors, the most important being the temperature of the ice, its internal structure and the conditions of loading. Because of these factors there is a wide variation in ice strength measurements quoted in the literature for thousands of tests on lake ice. The extreme range of results is shown in Table III.

Table III. Range of ice strength as measured.

Compressive strength	50 to 1800 psi
Flexural strength	44 to 414 psi
Shear strength	40 to 132 psi

The temperature of ice is one of the most important factors affecting its strength. Figure 18 gives the crushing strengths of strong clear lake ice and snow ice.⁷ The lake ice was columnar, made of prismatic crystals $\frac{1}{2}$ to 2 cm by 4 to 7 cm with the crystallographic c-axis nearly parallel to the surface of the sheet. The snow ice had small granular crystals $\frac{1}{2}$ to 2 cm in diameter with many air bubbles and a density from 0.82 to 0.87 g/cm³. Ten tests were made at each temperature. It can be seen that for a load applied parallel to the ice sheet with clear lake ice the strength was 177 psi at 32°F (0°C), 400 psi at 23°F (-5°C) and went as high as 1000 psi at -58°F (-50°C).

*In preparation.

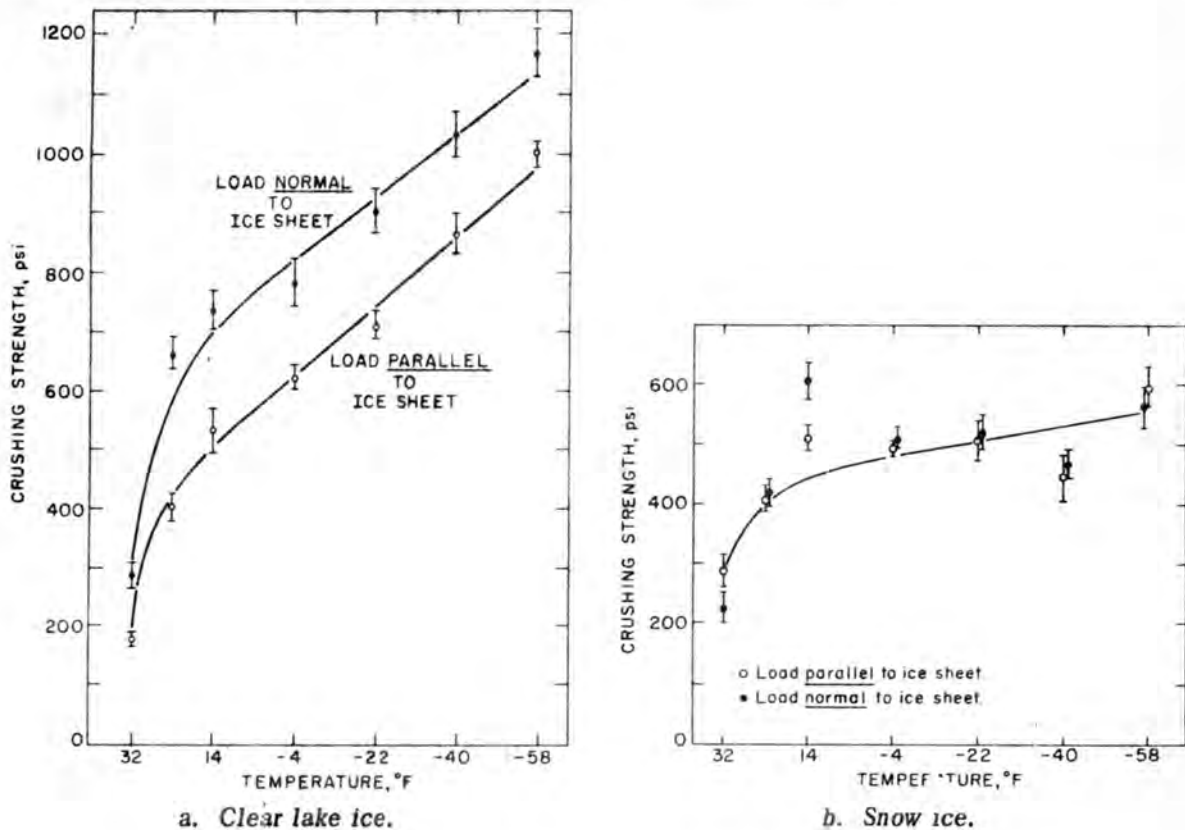


Figure 18. Crushing strength vs temperature of ice on Portage Lake, Michigan.⁷

The structure of ice also has a great influence on its strength. The quality of the melt is important because salts, gases and organic impurities sometimes collect, with air, at the boundaries of grains during their formation. The crystal structure - its form, dimensions and arrangement and the relative axis orientation of the grains - characterizes types of ice of widely different properties. The general faults in the structure such as stratification, cracks due to previous loading and thermal conditions, age and grain boundary melt (candling) play a dominant role in ice strength. This last factor bears particularly on the present application. It was found²⁸ that a combination of bright sun and air and ice temperatures near 32°F (0°C) will decrease the bending strength of ice by as much as six times from morning to midafternoon.

The strength of ice also depends on the conditions under which it is tested. The direction of stress application relative to crystal structure and the size of the specimens have an influence.⁹ The flexural strength of small beams is close to twice as high as that of bigger beams at the same location.²⁷ The rate of application and the duration of the load are also very important. Figure 19 shows the results of tests to determine the influence of the strain rate on the crushing strength for columnar ice with horizontal c-axes.¹²

To decide upon a value for the strength of ice in the design of isolated structures in lakes and rivers two different conditions may have to be considered. The first is the movement of ice floes by current and wind during the winter, especially in lakes where the ice sheet does not form over the whole surface. Under these conditions the temperature of the ice is, on the average, a few degrees below 32°F (0°C). It must be 32° at the ice/water interface and even in very cold weather it does

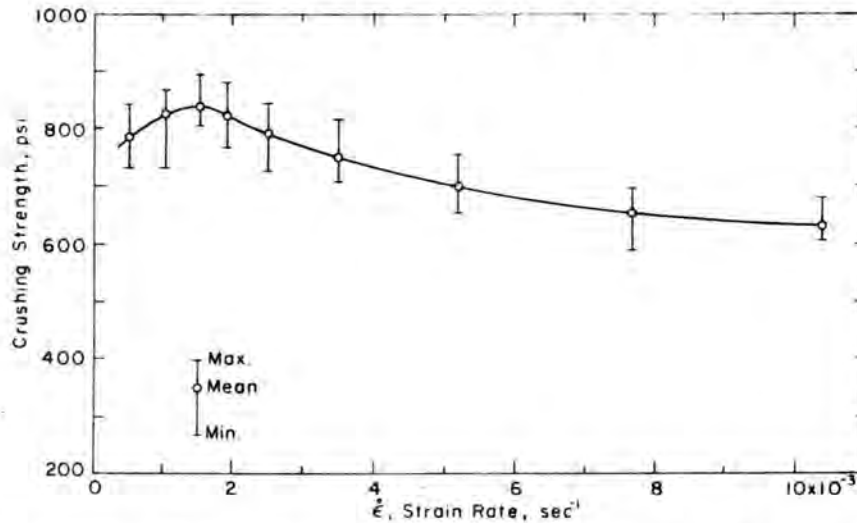


Figure 19. Influence of strain rate on the crushing strength of laboratory-made columnar ice with horizontal c-axes. Temperature: -10°F (-23°C).¹²

not usually get much below 32° at the surface because of the insulating effect of the snow cover. Besides, the temperature distribution is far from linear in the ice sheet itself, and the temperature in the upper layer is quickly attenuated toward 32° at the lower interface.

The second condition, the impact of ice floes at spring breakup, is the usual condition for the design of a bridge pier in a river. The water has previously flowed over the ice sheet, which has been considerably weakened by solar radiation before breaking up and moving down the river.

For these two conditions of winter and spring ice the strength values are chosen according to existing design values as given in Table IV for example.

Table IV. Design values of ice strength for impact loading.

	Winter ice	Spring ice
Compressive strength σ_0	400 psi	75 psi
Flexural strength σ_b	200 psi	65 psi
Shear strength τ_0	120 psi	60 psi

For winter ice strength design values should be taken for the strongest type of ice that can be produced in sizable area in a lake or a river. Unfortunately this is unknown at the present time but for clear lake ice with big prismatic crystals and little occluded foreign substances values of $\sigma_0 = 400$ psi and $\tau_0 = 120$ psi have been found at 23°F (-5°C).⁷ This crushing strength value of 400 psi is the same as that suggested by a Committee of the ASCE in 1931¹⁶ and introduced in the specifications of the AASHTO. The strength of ice in bending, Table IV, is suggested for small specimens of clear lake ice at 23°F .¹⁴ Before more is known about the strength of river and lake ice this may be used for design practice for a solid clear columnar ice sheet where by chance configuration no sensible flaw is present in the area under impact loading. Actual testing in nature with big ice beams shows a flexural strength which is normally lower.^{9 27 28}

The strength values for spring ice were taken directly from the highest values recommended by Korzhavin for rivers of the Northern U.S.S.R. and Siberia.⁴⁰ This is for ice floes moving at a speed of 3 ft/sec and the direction of the force essentially normal to the crystal prismatic axis. These values were obtained after standard testing and also by measurements of forces acting on piers.

Indentation of ice by a pier with vertical edge

The destruction of an ice floe by a pier with a vertical edge occurs in different ways, depending mostly on the stored kinetic energy of the floe and its strength. Upon impact with a pier a small ice floe is locally crushed, stops and then continues to move across an adjacent opening. A slightly larger floe generally collapses by splitting while a large ice field is cut without splitting. During the penetration of a pier into a large ice field, the width of indentation gradually increases and attains a maximum value equal to the total width of the pier, after which it remains constant.

General relationships. If we consider an ice floe hitting a pier, the energy transmitted to the obstacle is made up of the energy of deformation inside the ice floe and the energy required for its crushing. As the energy of deformation is negligible compared with the energy of crushing for sizable impacts, the fundamental relationship of mechanics gives:

$$F dx = m v dv \quad (8)$$

where F is the force exerted on the obstacle for a displacement dx of the floe, and m and v are the mass and instantaneous velocity of the floe.

On the other side, at crushing, we have:

$$F = \sigma_1 y h \quad (9)$$

where σ_1 is the crushing strength of ice by indentation, y is the width of the failure zone and h is the thickness of the ice.

For an ice floe, with an initial velocity V_0 , that is completely stopped by the pier we get, using eq 8 and 9:

$$\int_{x=0}^{x=x_0} h \sigma_1 (x) y (x) dx = \frac{1}{2} (m V_0^2). \quad (10)$$

Because of the geometry of the pier, the term on the left has an upper limit when $x = d_0$ and $y = B_0$ where d_0 is the length of the pier nose and B_0 is the total width of the pier.

If the kinetic energy in eq 10 is adequate to attain this upper limit, the floe will not stop and the maximum force will be given by:

$$H_{\max} = \sigma_1 B_0 h. \quad (11)$$

In the case where the indentation strength of the ice can be taken as independent of the indenter width x , the force required to stop an ice floe of a limited size can be easily computed:

$$A_0 = \int_0^{x=x_0} y (x) dx$$

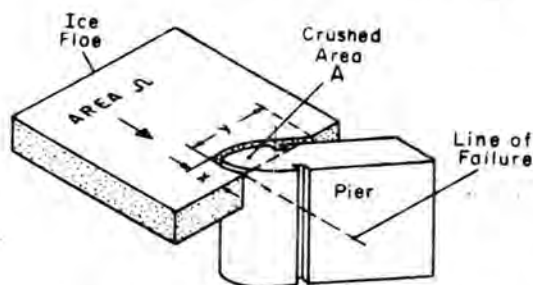


Figure 20. Crushing of an ice floe on a pier.

$$A_0 = \frac{m V_0^2}{2\sigma_1 h} \quad (12)$$

$$H = \sigma_1 y_0 h.$$

A_0 is thus the horizontal crushed surface of the ice floe when it stops as shown on Figure 20 and can be determined for any type of pier shape.⁴⁶ Actually, y_0 is the pier width corresponding to the A_0 area.

For the case of a triangular-nosed pier of angle 2α attacked by an ice floe along its axis we obtain the Petrunichev formula⁴⁶ for limited size floes:

$$H_{\max} = V_0 h \sqrt{2\rho\sigma_1 \Omega \tan \alpha} \quad (13)$$

where:

H_{\max} = maximum horizontal force, lb

V_0 = water velocity, ft/sec

h = ice thickness, ft

ρ = density of ice, 1.78 lbf-sec²/ft⁴

Ω = area of the ice floe, ft²

σ_1 = indentation strength of ice, lb/ft².

Strength of ice against indentation. The effect of the indenter dimensions on the strength of ice was studied experimentally by Korzhavin.⁴⁰ The ice used in the tests was taken from the river Ob at Novosibirsk. Its compressive strength was determined on 22 samples 70 × 70 × 70 mm at 32°F (0°C). The effect of load indentation was studied on 177 samples with sizes varying between 70 × 70 × 200 mm and 70 × 70 × 300 mm. The tests were performed as shown in Figure 21 and the following empirical relationship was proposed:

$$\sigma_1 = \sigma_0 \sqrt[3]{\frac{B}{b_0}} \quad (14)$$

where σ_0 and σ_1 are respectively the strength of ice in uniaxial compression and its strength with an indenter of width b_0 acting on an ice sample of length B . There is a limit to the value of B that can be used in the formula. For a large ice floe a complicated state of stress appears. Immediately following contact with the pier there is a zone of crushed material surrounded by zones of plastic, and elastic, deformation as shown on Figure 22. Taking the stress distribution of Boussinesq in the elastic zone, Korzhavin considers that the practical limit of induced stresses in the ice floe is given by the isobar corresponding to about 2 to 3% of the mean indenting pressure. The width B_1 of this isobar is approximately 15 b_0 , which can be taken as the effective width of large ice floes ($B > B_1$). Consequently when a large ice floe is cut by a pier the indentation strength cannot exceed the value:

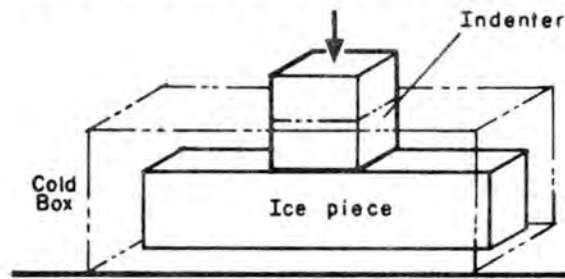


Figure 21. Indentation test.

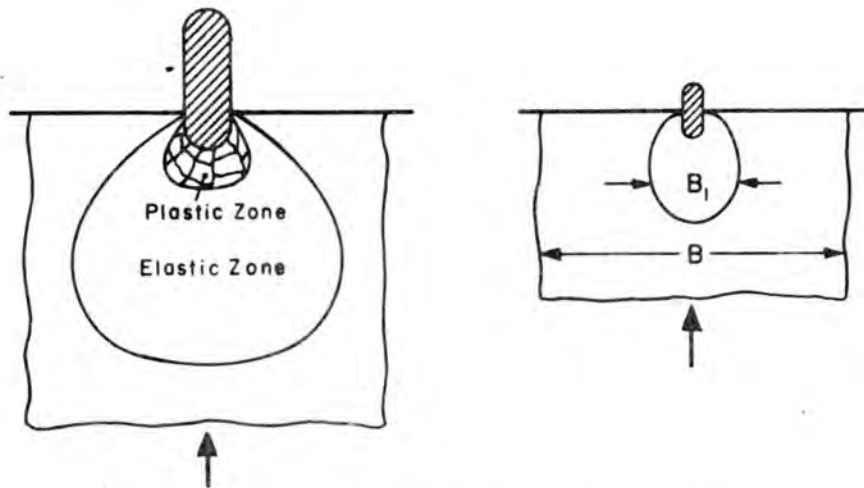


Figure 22. Stress zones in an indented block of ice.

$$\sigma_i = \sigma_0 \sqrt[3]{\frac{15 b_0}{b_0}} \cong 2.5 \sigma_0. \quad (15)$$

Influence of the rate of strain on the strength of ice. Tests carried out by G.A. Pchelkin, N.A. Tsytovich, and S.S. Vialov show that the strength of ice decreases with increasing strain rates. Korzhavin and Putkin⁴⁰ made a systematic study of this factor. The range of deformation studied on cube samples with 10-cm sides was from 2 to 32 cm/min. They found that the variation of strength of ice for rates of strain from 10^{-3} to 10^{-2} /sec could be expressed by the following empirical relation:

$$\sigma_i = \sigma_0 \sqrt[3]{\frac{\dot{\epsilon}_0}{\dot{\epsilon}}} \quad (16)$$

where $\dot{\epsilon}$ is the axial strain rate in the sample and $\dot{\epsilon}_0$ is a reference value of this rate when $\sigma_i = \sigma_0$.

When ice floes hit piers under natural conditions, the strain rate decreases with the distance from the pier. In the first approximation, only the plastic zone of deformation may be considered and on the basis of ice indentation tests performed by Korzhavin this zone would be 1.5 to 2.0 times

the width of the indenter, here B_0 , the pier width. If the velocity of the ice floes is V_0 ft/sec and the length of the plastic zone $L_0 = 2B_0$, the mean strain rate in that zone is:

$$\dot{\epsilon} = \frac{dL_0/L_0}{dt} = \frac{V_0}{2B_0} \quad (17)$$

For the same pier width the strain rate is proportional to the velocity of the floe in the range where eq 15 would be applicable. Extrapolating to higher rates of stress application, Korzhavin proposed the final formula:

$$\sigma_i = \sigma_0 \sqrt[3]{\frac{V_0}{V}} \quad (18)$$

where V_0 is a reference velocity of 3.3 ft/sec (1 m/sec).

Because other experimenters have found that ice strength does become relatively constant for higher rates of loading,^{9 12 27} a range not tested by Korzhavin, the author believes that this correction on the strength of ice should not be taken into consideration until further measurements are made.

Influence of contact between the flowing ice and the pier. Because of the brittle fracture of ice floes, there is never a complete contact between the pier surface and the ice. The effective length of the contact surface between the ice and the pier can be taken as:

$$B = \zeta B_0 \quad (19)$$

where B is the effective contact width and ζ is a reduction coefficient which, according to Korzhavin, shall be taken between 0.4 and 0.7 for ice of medium strength as in Table V.

Table V. Values of contact coefficient ζ according to Korzhavin.

Pier width (ft)	Velocity of ice floes, ft/sec		
	1.5	3.3	6.6
10-17	0.70	0.60	0.50
20-27	0.60	0.50	0.40

Influence of the form of the indenter. The shape of the cutting edge of the indenter influences the strength of ice considerably according to experimental investigations made by Korzhavin. He studied the effect of six different indenter shapes: semicircular, flat and wedge shapes, the latter with wedge angles $2\alpha = 120^\circ, 90^\circ, 75^\circ$ and 60° . The tests were made at 32°F (0°C) and the rate of indentation was 1.5 cm/min. Altogether 73 tests were made of which 52 were with lateral confinement.

The experimental results can be summarized as follows:

1. The shape of the crushed zone near the indenter depends on the shape of the indenter. For flat indenters it is semicircular. For wedges, the size of the zone decreases with decreasing wedge angles and it disappears completely for wedges of $2\alpha = 60^\circ$.

2. The pressure on the ice caused by the indenter increases continuously but irregularly with penetration. At the instant of cracking, the pressure falls and the load has a vibrating character.

3. The indentation of ice produces mostly a brittle failure with crack formation.

4. For computing the pressure of large ice floes on piers, Korzhavin recommends the use of a shape factor ζ' whose values are given as follows:

- a. for flat-edged piers ($2\alpha = 180^\circ$), $\zeta' = 1.0$.
- b. for semicircular-edged piers, $\zeta' = 0.90$
- c. for wedge-shaped piers ($60^\circ < 2\alpha < 120^\circ$), $\zeta' = 0.85 \sqrt{\sin \alpha}$. (20)

Korzhavin's formula for indentation. The basic formula (eq 11) still applies if the crushing strength of ice by indentation is obtained from the previous considerations. We then have:

$$H_{\max} = \sigma_i B_0 h \quad (11)$$

where

$$\begin{aligned} \sigma_i &= \zeta \zeta' \sigma'_0 \\ \sigma'_0 &= \sigma_0 \sqrt[3]{\frac{B}{B_0}} \text{ for } B < 15 B_0 \\ \sigma'_0 &= 2.5 \sigma_0 \text{ for } B > 15 B_0 \end{aligned} \quad (21)$$

When the kinetic energy of the ice floe is not high enough to develop the maximum pressure, relation 10 also applies but in that case it must be recalled that σ_i is no longer a constant but a function of the pier penetration according to eq 21. The area Ω_c of the ice sheet required to develop the maximum pressure can be determined. For a triangular nose of angle 2α , the integration of eq 10 leads to:

$$\frac{1}{2} (m V_0^2) = 0.95 \zeta \zeta' h \sigma_0 \sqrt[3]{B X_0^5 \tan^2 \alpha} \quad (22)$$

which for $X_0 = B_0/2 \tan \alpha = d_0$ gives:

$$\frac{1}{2} (m V_0^2) = 0.6 H_{\max} d_0 \quad (23)$$

where d_0 is still the length of the cutting edge of the pier. The critical size of the ice floe required to develop this maximum pressure is:

$$\Omega_c = \frac{0.6 \zeta \zeta' B_0^2 \sigma_0^2}{\rho V_0^2 \tan \alpha} \quad (24)$$

For a wide floe, $B > 15 B_0$, this is:

$$\Omega_c = \frac{1.5 \zeta \zeta' B_0^2 \sigma_0}{\rho V_0^2 \tan \alpha} \quad (25)$$

Thus for average values of the parameters, relatively small floes of 100×100 ft to 300×300 ft are required to develop the maximum ice pressure. The force that a smaller floe exerts when stopping in front of the pier can be readily found from eq 12. For a triangular-nosed pier, it is:

$$H_{\max} = 1.29 V_0 h \sqrt{\rho \sigma_1 \tan \alpha} \quad (26)$$

which is not much different from Petrunichev's formula (eq 13).⁵⁶ For a semicircular pier nose the same equation can be used in which Korzhavin proposes to take an equivalent wedge of angle $2\alpha = 140^\circ$.

Splitting of ice floes by a pier with a vertical edge

We will now consider the case of an intermediate-size floe which is neither stopped by the pier nor crushed but is split along a line of minimum resistance. The minimum resistance may be given either by shear at an angle on both sides of the pier or on the axis of the pier, or by tension cracks forming in the floe.

Shear cracks. Let us consider a floe of size $L \times B \times h$ (Fig. 23) whose size is not big enough to attain the critical value Ω_c given in eq 24. The shape of the failure crack can be taken as a straight line. Contact forces between the pier and the floe can be reduced to two normal forces T and two friction forces F . For equilibrium conditions:

$$P - 2T \sin \alpha - 2F \cos \alpha = 0. \quad (27)$$

Because we have:

$$F = f T$$

where f is the friction coefficient of ice on the pier surface, we obtain:

$$T = \frac{P}{2(\sin \alpha + f \cos \alpha)} \quad (28)$$

Assuming the length of the crack S_1 we get along the line of shear failure:

$$T(\cos \theta + f \sin \theta) = h S_1 \tau_0 \quad (29)$$

where τ_0 is the average splitting stress in the section corresponding to the shearing strength of the ice. It is evident that such an averaging process is permissible only for relatively small floes. Neglecting friction forces in the first approximation we get:

$$P = \frac{2\tau_0 h S_1 \sin \alpha}{\sin(\alpha + \beta)} \quad (30)$$

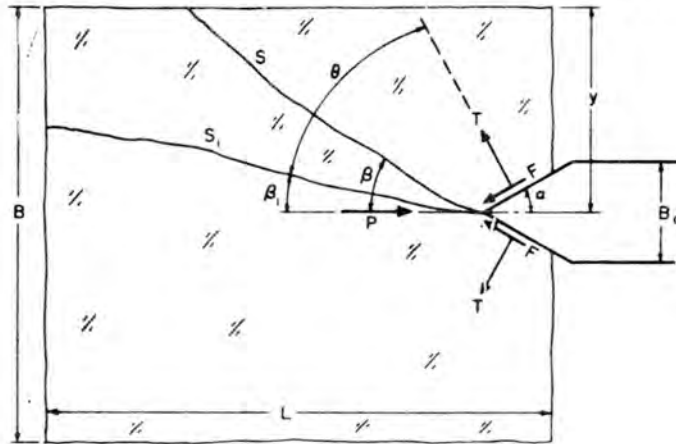


Figure 23. Splitting of an ice floe by a pier having a vertical edge.⁴⁰

When the crack reaches the side of the floe, we have $S_1 = (B/2) \sin \beta$. The force P becomes:

$$P = \frac{\tau_0 h B \sin \alpha}{\sin \beta \sin (\alpha + \beta)}. \quad (31)$$

The splitting occurs for P_{\min} , when:

$$\beta = (90^\circ - \alpha).$$

And the maximum axial force acting on the pier with this lateral splitting is:

$$H_{\max} = 2\tau_0 B h \tan \frac{\alpha}{2}. \quad (32)$$

If the floe is not long enough, the minimum value of the force is attained with a longitudinal crack in the axis of the pier and this force is then:

$$H_{\max} = 2\tau_0 L h \sin \alpha. \quad (33)$$

Splitting of small floes by tension cracks. For small ice floes and very sharp-edged piers, a splitting failure due to normal tensile stresses at the crack is possible. According to Korzhavin the following expression is suggested for that case:

$$\beta = \frac{\alpha}{2} \quad (34)$$

$$H_{\max} = n L h \sigma_t$$

where σ_t is the tensile strength of ice and n is a shape factor for the pier varying as a function of the wedge angle according to Table VI.

Table VI. Shape factor, n , and pier angle, 2α .⁴⁰

Pier angle 2α	60°	70°	80°	90°	100°	120°
n	0.25	0.29	0.33	0.38	0.43	0.53

In all cases of floe splitting, the force on the pier is always smaller than the maximum force required to crush the ice by complete indentation through the floe. Thus in the case of large floes the splitting is always partial with the formation of cracks of limited length.

Failure of ice floes on inclined piers

Inclining the cutting edge of a pier produces an important decrease in the horizontal component of the pressure and the appearance of a vertical component. This facilitates the work of ice cutting and greatly increases the stability of the pier.

After a floe contacts the inclined edge of a pier, its lower sharp edge is crushed and a reaction appears, as shown in Figure 24, which can be decomposed into two forces V and T as:

$$V = T \cot \beta. \quad (35)$$

Under the action of these components the floe can fail in three different ways:

1. by bending in section 1-1
2. by shearing in section 2-2
3. by crushing under the forces T , which are equal to:

$$H = 2T \sin \alpha. \quad (36)$$

The type of failure that takes place depends on which kind of stress attains its ultimate value first. It can be shown that failure by shearing is the most probable at breakup. As is known, the ice cover of rivers and lakes represents mainly an agglomerate of vertically oriented crystals, separated from one another by narrow layers where impurities can collect. During the spring thaw the resistance of ice to sliding along these crystal faces is much reduced. Observations in nature show that failure by shear occurs in the immediate vicinity of the pier, so that a channel of crushed ice of width B_0 remains behind the pier.

If the process of spring thaw is not yet sufficiently developed, a bending failure of the ice cover is possible. In that case too the fracture occurs in the vicinity of the pier at a distance not exceeding 3 to 6 times the thickness of the ice cover. The width of channel formed by the pier in the ice field is larger than in the previous case, but is still only a little larger than the pier.

Fracture by crushing is possible only for rigid piers when the vertical component is small.

Failure of large ice floes by shearing. It is assumed that at the moment of shear failure the edge of the floe has already been crushed to a length z (Fig. 24). Investigations show that failure occurs at the pier surface where z is small. We then find

- a) The length of the shear surface:

$$b_s = \zeta \Pi \quad (37)$$

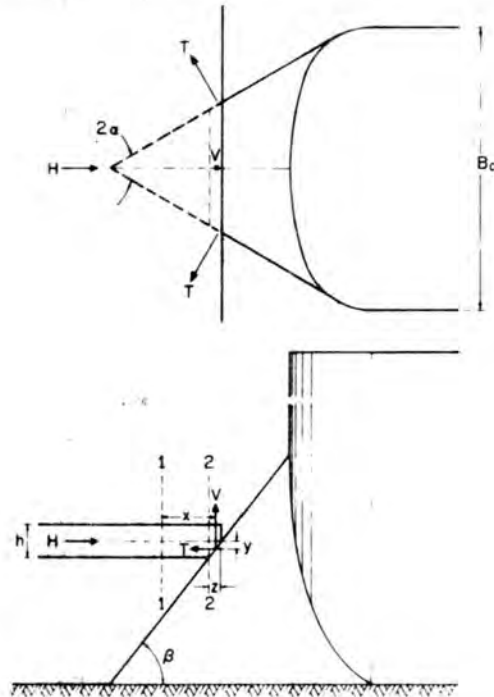


Figure 24. Failure of ice on the inclined edge of a pier.⁴⁰

where Π is the perimeter of the cutting edge of the pier and ζ is a coefficient of contact.

b) The greatest possible vertical force acting on one-half of the pier:

$$V = \frac{b_s h r_0}{2} \quad (38)$$

c) The greatest possible horizontal force:

$$T = 1.1 V \tan \beta_1 \quad (39)$$

The coefficient 1.1 is introduced, according to current practice,⁷⁵ to take account of dynamic friction forces between the pier and the ice floe. β_1 is the angle of inclination of the sides of the cutting edge to the horizontal:

$$\tan \beta_1 = \frac{\tan \beta}{\sin \alpha} \quad (40)$$

d) The greatest possible horizontal force acting on the whole pier:

$$H_{\max} = 2 T \sin \alpha = 2.2 V \tan \beta \quad (41)$$

For a pier with a wedge-shaped cutting edge the maximum possible length of the shear surface can be found from the relation:

$$b_s = \frac{\zeta B_0}{\sin \alpha}$$

and the calculated forces on the whole pier are equal to:

$$V_{\max} = \frac{\zeta B_0 h r_0}{\sin \alpha} \quad (42)$$

$$H_{\max} = \frac{1.1 \zeta B_0 h r_0 \tan \beta}{\sin \alpha} \quad (43)$$

In the case of a semicircular cutting edge we get:

$$V_{\max} = \frac{\pi}{2} \zeta B_0 h r_0 \quad (44)$$

$$H_{\max} = \frac{1.1 \pi}{2} \zeta B_0 h r_0 \tan \beta \quad (45)$$

where in both cases the contact coefficient ζ can be taken as in the case of ice crushing (Table V).

Failure of large ice floes by bending. This case might theoretically be investigated with the theory of a plate lying on an elastic foundation, as the inverse problem of the bearing capacity of an ice sheet. This theory shows that the failure of the ice sheet begins with the formation of radial cracks starting from the load and the collapse occurs when a circumferential crack develops. This latter condition gives the maximum loading condition on a pier. However, observations by Korzhavin do not substantiate the theory for this application.

The plate theory is derived for vertical loading only. Here the horizontal component of the force on the pier combines with the vertical one to modify the stress distribution. The theory is applied for a uniformly distributed load over a circular area. Here we have peripheral loading along different shaped pier noses and observations show that these forms are a prime factor affecting the ice pressure.

In elastic deformation the theory shows that the circumferential crack would appear at a distance on the order of twenty times the thickness of the sheet while observations by Korzhavin show that the dimensions of broken pieces of ice do not exceed 3 to 6 times this thickness, and are frequently smaller. In the theory of the ideal plastic plate the position of the circumferential crack has to be indirectly assumed.

We will thus present here Korzhavin's semi-empirical derivation where the main hypothesis is that the collapse of the ice sheet occurs at a distance of $3h$ from the sides of the piers. This distance was also chosen because it is safe for engineering design, since it gives a higher force than could probably act.

When an ice floe contacts a massive pier, indentation occurs first when the lower edge of the floe is crushed. The ice then comes in contact with the side of the pier, a vertical and horizontal reaction is set up, and the ice is ruptured with the formation of at least three radial cracks as shown in Figure 25. These radial cracks are followed by transverse cracks breaking a piece of the floe of form 1-2-3-4. After that, the force on the pier is reduced until a new contact is restored and the same process continues. In this manner, the resulting reaction of the pier on the ice floe is reduced to two forces on each side, V and T (Fig. 24).

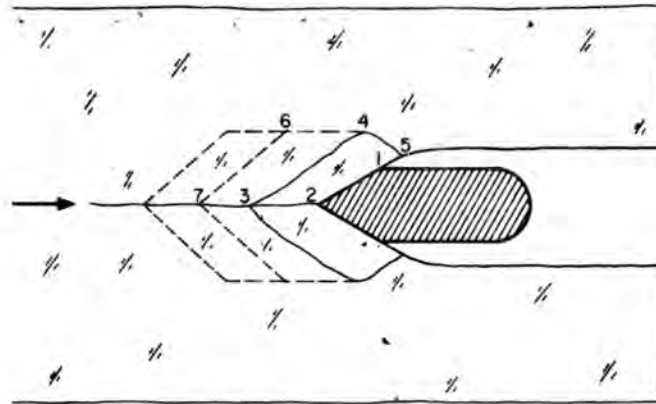


Figure 25. Progressive bending failures of an ice sheet at an inclined edge of a pier.⁴⁰

Again taking into account the dynamic friction force of ice against the structure with a coefficient $f = 0.1$, we get:

$$H = 2 T \sin \alpha \quad (45)$$

$$H = 2.2 V \tan \beta. \quad (47)$$

As the separation of the ice into two strips precedes its breaking, the greatest pressure on the ice occurs at the moment of failure along the line 3-4. The length of this line can be written:

$$l_{34} = \frac{n_0 B_0}{2 \sin \alpha} \quad (48)$$

where n_0 is a coefficient higher than unity taking into account the plan-shape of the pier. Korzhavin considers the strip 2-3-4-5 as a finite element clamped in section 3-4 and acted upon by forces V and T at the other end. The element being short ($3h$) and its deformation small before failure, its weight and hydrostatic reaction are neglected in relation to the breaking forces. The bending moment in section 3-4 is then given by:

$$M = V x - T y. \quad (49)$$

Because there is no deep indentation of the ice floe (Fig. 24) the forces V and T are not applied at the center of the ice sheet but near its lower surface. Korzhavin arbitrarily proposed to take $y = 0.25 h$ for this point of application. At failure the yield moment of ice for an elastic plate is:

$$M_0 = \frac{\sigma_b h^2 l_{34}}{6} \quad (50)$$

where σ_b is the flexural strength of ice.

With these relations and the basic hypotheses $x = 3h$ and $y = 0.25 h$, the total forces acting on the pier are found to be:

$$H_{\max} = C_0 \sigma_b h \tan \beta B_0 \quad (51)$$

$$V_{\max} = 0.9 C_0 \sigma_b h B_0 \quad (52)$$

and

$$C_0 = \frac{0.73 n_0}{12 \sin \alpha - \tan \beta} \quad (53)$$

Assuming a similarity between the bending and indentation mechanisms, Korzhavin finds a relation between the coefficient n_0 and the angle of the pier 2α . Adjusting its value so that it will fit experimental data, he finally proposes:

$2\alpha - 45^\circ$	60°	75°	90°	105°	120°
$n_0 - 0.94$	1.18	1.42	1.68	1.98	2.0

The values of C_0 can then be determined from eq 53 (Table VII).

Table VII. Values of coefficient C_0 .

β	$2\alpha = 45^\circ$	60°	75°	90°	120°
45°	0.20	0.17	0.16	0.16	0.15
60°	0.24	0.20	0.19	0.18	0.17
70°	0.38	0.27	0.23	0.21	0.19
75°	0.79	0.38	0.29	0.26	0.22

It can be seen that the influence of the angle 2α becomes important at small values ($2\alpha < 60^\circ$). An increase of H_{\max} for small angles 2α can be explained by the fact that a sharper pier penetrates farther into the floe and the length of broken pieces is correspondingly increased. If the cutting edge is rounded in plan, some additional cracks appear; Korzhavin then recommends taking the rounded edge as approximately equivalent to a sharp edge as shown in Figure 26 whose angle α is given by the formula:

$$2\alpha = 2\alpha_1 + \frac{4r}{B_0} (40^\circ - \alpha_1) \quad (54)$$

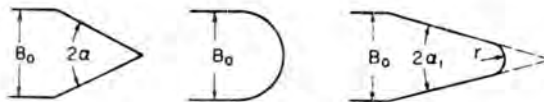


Figure 26. Round edge and equivalent angle of a sharp-edged pier.⁴⁰

Verification and utilization of method

The method of evaluation of the force of impact of ice floes as proposed by Korzhavin has been verified in nature by a kinematic method. Knowing the mass of an ice floe and its change in velocity during its action on a structure, it is possible with basic laws of mechanics to determine the reaction of the structure. This was done by taking into account the boundary shear force of the flow and the component of weight of the ice floe as given by the slope of the free surface of the river. The results of these field measurements compared to computed values are shown in Table VIII.

Table VIII. Measured and calculated ice thrust.⁴⁰

Data	Unit	Year of measurement					
		1933	1954	1955	1959	1956	1960
No. of ice floe		1	2	3-5	6-9	10-11	12-15
Area of ice floe	1000 m ²	15.6	2.5	24.0	0.7	3.6	3.6
Size and shape of pier							
Width (B ₀)	m	4.4	4.4	4.4	4.0	7.7	3.4
Roundness (radius r)	m	1.0	1.0	1.0	2.0	0.0	0.6
Sharpness (angle 2α)	deg	48	46	46	80	115	83
Inclination (angle β)	deg	57	57	57	45	90	90
Measured force (H _{max})	tons	45.8	17.5	46.4	15	63	28
Calculated force (Korzhavin)	tons	72.5	25.5	54.5	27	108	70
Thickness of ice (h)	m	0.98	0.50	0.90	0.85	0.50	0.70

Note: In 1954 and 1960, the ice strength was lower than usual.

The calculated values are in general greater than the measured ones. It is always very difficult to make adequate verification in the field because of the extremely variable strength of ice during the spring breakup. To our knowledge the maximum force acting on a pier has rarely been measured by a direct method in nature. With a dynamometric plate of small size, Korzhavin found a maximum of 130 psi for σ_i during a spring breakup and the Alberta Research Council, in similar circumstances, found a maximum pressure $\sigma_i = 100$ psi. This is definitely compatible with design values of ice strength suggested by Korzhavin. For such plates the contact coefficient would probably be 0.6 and the computed design indentation strength would be $\sigma_i = 113$ psi (cf. the measured value of 100 psi).

To summarize the results of the Korzhavin method it might be considered that the force exerted on a pier is the smallest of that necessary to break the ice either by crushing, bending or shearing as computed by the following equations:

- 1) Indentation failure for all types of piers:

$$H_{\max} = 2.5 \zeta \zeta' \sigma_0 B_0 h \quad (55)$$

with ζ given in Table V and ζ' on page 26.

2) Shearing failure for an inclined pier:

$$H_{\max} = 1.1 \zeta B_0 h \tau_0 \frac{\tan \beta}{\sin \alpha} \quad (43)$$

3) Bending failure for an inclined pier:

$$H_{\max} = C_0 \sigma_b h B_0 \tan \beta \quad (49)$$

with C_0 given in Table VII.

In those formulas, H_{\max} is the maximum horizontal force in pounds; σ_0 , σ_b and τ_0 are the crushing, bending and shearing strengths in psi; h and B_0 are the ice thickness and pier width in inches and finally ζ , ζ' , C_0 are dimensionless coefficients.

In the case of an indentation failure it is necessary to check (eq 25) to see that a floe of the required size, having the required energy to attain complete indentation, can exist. This size is limited by river characteristics, spacing of piers, etc.

We emphasize the fact that sloping a pier nose is the most effective way to reduce the horizontal force caused by ice impact. For a pier nose with a horizontal angle $2\alpha = 90^\circ$, an inclination of $\beta = 45^\circ$ will reduce the horizontal force as much as tenfold with the usual values of the parameters. Furthermore, the vertical component of this force then contributes to the stability of the pier. Finally, the possibility of jamming by bigger floes stopping and arching between the piers is then much reduced.

The influence of the horizontal angle of the pier nose is not straightforward. For a vertical edge pier nose, the sharper it is, the more effective it is for cutting ice. The reduction of the angle from $2\alpha = 120^\circ$ to $2\alpha = 60^\circ$ would reduce the horizontal force on the pier by about 25%. However, the effect is in the opposite direction for an inclined pier nose and a sharpening of the angle increases the force on the pier because longer strips of ice have then to be broken on both sides by bending.

Miscellaneous effects of moving ice

Abrasive action of ice. When an ice pack is moving either during breakup or during wintertime, the floes may come in close contact with wharves, piers, retaining walls or dams and may cause abrasion of the structures at the water level. Deep cuts in a wall, on the order of a foot, have brought about the collapse of a wharf.¹⁴ Piles have been cut in less than five or six hours.¹⁶ Recently, during a spring breakup, concrete walls were locally eroded to a depth of about 1 to 3 in.¹⁷

The erosion of river shores by moving ice is well known and may be much more severe in northern countries than scouring action by water alone. Even rock banks are extensively eroded by ice. One of the main drawbacks of shore protection with boulders, artificial blocks, sand bags, etc. is their poor resistance to ice abrasion. This action is particularly severe on concave river banks and an interesting solution has been used recently in Minneapolis on the Mississippi River. A log boom was attached at the upstream end of a bend and allowed to swing free; it stabilized at a certain distance from the bank because of the spiral motion of the flow. Ice floes tending to hit the bank were deflected by the boom, whose inertia, together with the inertia of the water behind it, easily guided the ice out, avoiding the bank (Figure 27).

The maximum local pressure that ice can exert while moving along a longitudinal structure corresponds to local crushing of the ice. The normal component to the structure face can be



Figure 27. Ice boom deflecting ice. Mississippi River at Elk River.

computed from the previous indentation formula, with no increase in this case for the size of the indenter:

$$\sigma_n = \zeta \sigma_0. \quad (56)$$

The longitudinal pressure of the moving ice is the dynamic friction force:

$$\tau = \sigma_n f \quad (57)$$

with $f = 0.1$.

These are in effect localized point loadings and should not be applied simultaneously over the whole wall surface. Because of their repetitive character, abrasion results in the long run. That is why it is recommended that the surfaces of structures subjected to severe ice conditions of that type be hardened either by using special surfacing concrete or by adding extra protection such as granite or steel revetments.

In some cases the design of low slope lateral works may be advised. An ice foot will then form and remain in place at breakup time to take up the impact of moving ice.

Ice accumulations. A moving ice field may, under the action of water currents or winds, hit the shore of a lake or river and any engineering work located there. It will then induce important ice accumulations while slowing down, and dissipating its energy by breaking and accumulating smaller ice pieces on its edge. Figure 28 shows an accumulation of more than 25 ft on the shore of Lake Erie. Accumulations of this size have repeatedly been reported in the literature and one close to 100 ft high³⁹ has been observed

These accumulations may have harmful effects on installations and works merely because of their bulk but the total force they exert is usually considerably smaller than the initial impact of the ice on the structure. When at rest the force they exert may be estimated by simulating the accumulation of a granular soil. The horizontal pressure at any point above the water surface is then given by (Fig. 29).



Figure 28. Accumulation of ice on the shore of Lake Erie.

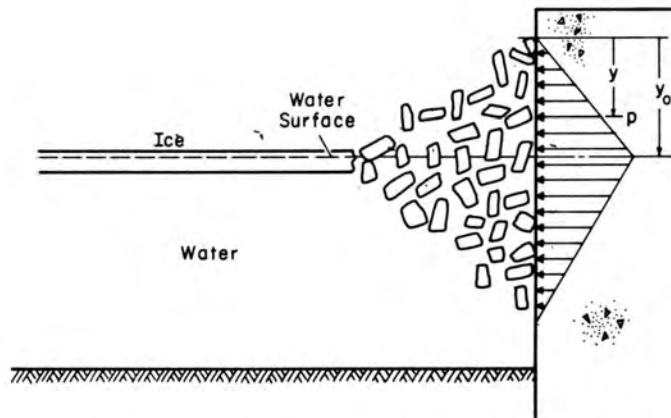


Figure 29. Horizontal pressure of ice accumulation against a vertical wall.

$$p = K_a \gamma' (1 - e), \quad y < y_0 \tag{58}$$

where

$K_a = \tan^2 (45^\circ - \frac{\phi}{2})$, the coefficient of active pressure of the ice pieces

y = height of ice on top of the considered point

ϕ = angle of internal friction of the ice pieces

γ' = unit weight of ice

e = porosity of the ice accumulation (ratio of voids to total volume).

Under the water surface, the pressure decreases and is given by:

$$p = K_a [\gamma_0 \gamma' (1 - e) - (y - y_0) (\gamma - \gamma') (1 - e)] \quad (59)$$

for $y > y_0$

where γ is the unit weight of water.

The difficulty lies in assuming reasonable values for e and ϕ . The densest ice pack with snow and slush accumulation between the solid ice pieces would not have an e value sensibly smaller than 0.9. The value of ϕ may be estimated by noticing that most of these ice mounds have an angle of repose close to 30° .

Ride-up of ice on bridge piers. On a pier with a sloping face the broken floes may ride up the face to a certain level before falling off. If there is insufficient clearance between the water and the bridge deck, they may occasionally hit the superstructure and cause damage.

Because a floe of any possible form pushed by a large ice field may occasionally hit a pier we have to consider the longest floe that can ride up the face of the pier without breaking. It was found⁴⁵ that a floe having the form of a thin beam, simply hinged and pushed by a large field, would be the more resistant to a ride-up. With most of the floe length out of water, the critical length was computed from equilibrium conditions:

$$L_c = 1.07 \sqrt{\frac{8 M_b}{\gamma' h}} \quad (60)$$

$$\alpha_c = 25^\circ$$

where M_b is the resisting moment per unit width for the ultimate strength of ice

$$M_b = \frac{\sigma_b h^2}{6}$$

and α_c is the critical angle at which the floe is most apt to break. For values of σ_b of 65 psi at breakup the critical length is given by:

$$L_c = 15.8 \sqrt{h} \quad (61)$$

where L_c and h are in feet. When this length is laid along the inclined face of the pier it gives the maximum possible rise before the floe falls away.

VERTICAL FORCES EXERTED BY ICE ON HYDRAULIC STRUCTURES

Introduction

Among the forces exerted by ice on hydraulic structures, one of the least known, and perhaps most often neglected in design practice, is the vertical force transmitted to a structure by an ice sheet during water level fluctuations.

The adhesive strength of ice on various construction materials is high and considerable moments and forces have to be resisted by the walls of structures following a variation in water

level. With a rise in the level, piers, caissons, pile groups, well casings and even rectilinear wharf sheetings may be partly lifted off their foundations and damaged. Observations in northern Sweden have shown that even large caissons can be lifted by the ice and one was raised more than 20 cm (8 in.).⁴² Damage can also be inflicted on revetments, gates or protruding parts of dams and intake works frozen in the ice sheet, following the usual lowering of the reservoir level during winter operation.

The theoretical determination of the vertical force exerted by an ice sheet is a difficult task for a number of reasons.

The first difficulty arises because water level fluctuations occur frequently during the winter. The initial failure produced in a thin sheet becomes the weak point where subsequent failures will be located. This time-dependent phenomenon defies analysis and is particularly apparent in tidal waters where high ice caps build up on the upright surfaces of structures. Fortunately these caps do not usually have extensive horizontal projections and the computation can be carried out as with the original boundary if the maximum thickness of the solid ice sheet that can be formed with a stable water level can be predicted.

Another difficulty is our limited knowledge of the basic creep properties of ice of various types of internal structure and qualities of the melt, and our inability to predict them at each particular site.

Finally, not one of the smallest problems is the complexity of the analysis of the basic behavior of a floating ice sheet subject to very slowly applied loads, if the viscoelastic properties of the ice have to be taken into account. Many approximate assumptions have to be made to get usable answers. One is to use the theory of elasticity with brittle failure of ice. The other method is to determine the maximum loading conditions for the ultimate strength of ice on the basis of plastic theory. In this latter connection it might be said that analyses pertaining to the similar problem of the bearing capacity of an ice sheet are most useful and have been applied to this case.

Lifting force on isolated structures

Elastic behavior under concentrated loading. The case of a rising ice sheet attached to a pier or a pile can be ideally represented by the similar one of a concentrated load applied to a large floating sheet of uniform thickness.

The first approach to the solution of this problem is the use of the theory of elastic deformation of an infinite plate on an elastic foundation. This solution was first obtained by Hertz⁴³ for the case of a concentrated load.

The equation of the deflection w of such a plate is:

$$\left(\frac{d^2}{dr^2} + \frac{1}{r} \frac{d}{dr} \right) \left(\frac{d^2 w}{dr^2} + \frac{1}{r} \frac{dw}{dr} \right) = \frac{q - sw}{D} \quad (62)$$

where q is the external load applied to the sheet, s is the foundation modulus, and D is the flexural rigidity of the plate:

$$D = \frac{E h^3}{12 (1 - \nu^2)}$$

in which:

E = modulus of elasticity of the plate

h = plate thickness

ν = Poisson's ratio, which is usually taken as $\frac{1}{2}$ for ice.³²

The complete solution of the Hertz problem has the form:

$$w = \frac{PL^2}{2\pi D} \operatorname{kei} \frac{r}{L} \quad (63)$$

where L is the characteristic length or radius of relative stiffness:

$$L = \left[\frac{Eh^3}{12(1-\nu^2)s} \right]^{\frac{1}{4}}$$

and the function kei is a Kelvin function of zero order.¹⁵

At the origin we have $\operatorname{kei}(r/L) = -\pi/4$ and the deflection under the load becomes:

$$w_{\max} = \frac{PL^2}{8D} = \frac{P}{8sL^2} \quad (64)$$

The distribution of the unit bending moments due to the concentrated load is given by:

$$\left. \begin{aligned} M_r &= \frac{P}{4} \left[(1+\nu) \left(\ln \frac{2L}{r} - 0.577 \right) - \frac{1}{2} (1-\nu) \right] \\ M_t &= \frac{P}{4} \left[(1+\nu) \left(\ln \frac{2L}{r} - 0.577 \right) + \frac{1}{2} (1-\nu) \right] \end{aligned} \right\} \quad (65)$$

The radial moments become negative at some distance from the load, their numerically largest negative value being about $-0.02P$ at a distance r close to $1.9L$. The tangential moments are always positive, being infinitely large at the origin and getting asymptotically equal to zero at an infinite distance from the center.

If the concentrated load is applied over a small circular area of radius a , the moments take a finite value under the load.⁷¹ As the load increases, the bending stresses below it become equal to the flexural strength of the ice and the sheet begins to yield, leading to radial tension cracks at the bottom (Fig. 30).

Circumferential collapse of the ice sheet. After radial tension cracks have appeared in an ice sheet submitted to concentrated loading the deflection of the sheet increases quickly until the bending stresses along a circumferential section become equal to the flexural strength of the ice and a circumferential tension crack is formed on the top (Fig. 30). The ultimate bearing capacity or collapse load of the sheet is then reached. One first method of analysis is to consider an elastic, homogeneous, isotropic material for the floating ice sheet that has been cracked in several radial sections. The stress distribution in such a sheet has been completely solved.⁵⁰ The load leading to the circumferential collapse has been obtained for various values of the radius a of loading and a Poisson's ratio of $\frac{1}{2}$ for ice (Fig. 31).

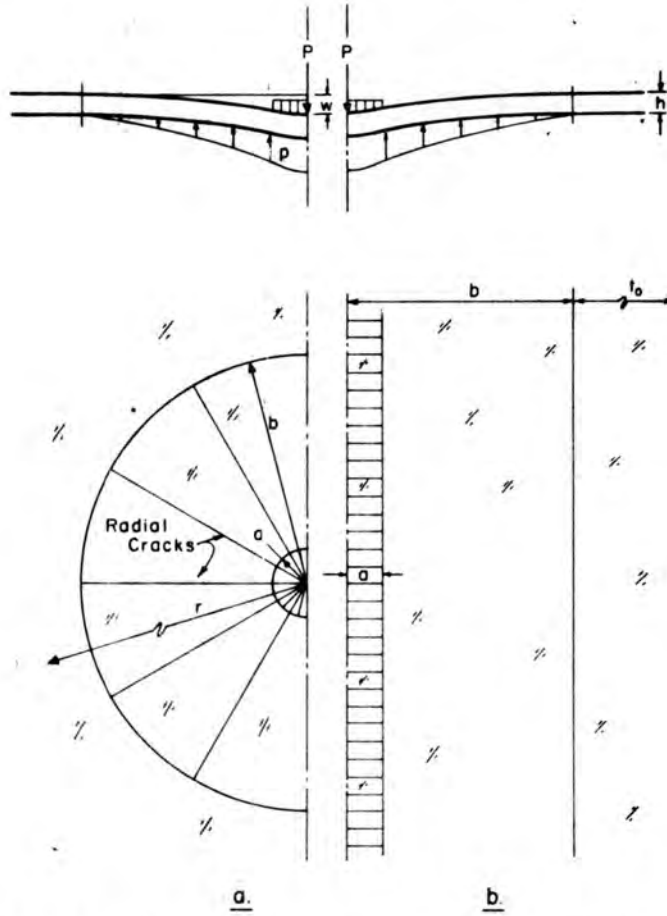


Figure 30. Infinite plate under load. (After Meyerhof.⁴⁴)

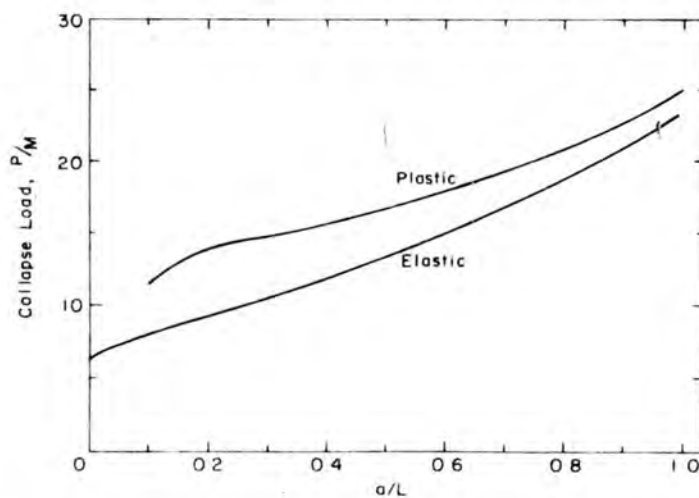


Figure 31. Elastic and plastic failures of a radially cracked ice sheet.

Another way to determine the theoretical collapse load is to assume⁴⁴ that the ice sheet is a thin, rigid, ideally plastic infinite sheet which can, without cracking, resist a full plastic limit bending moment per unit length, $M_0 = \sigma_0 h^2/4$, where σ_0 is the yield strength of the material in tension. At very low rates and long duration of stressing, the strain capacity of ice is large, as shown by creep tests. Meyerhof⁴⁴ says, therefore, that in this case the moment-rotation capacity of ice in bending is adequate to enable the limit moment M_0 (using the plastic section modulus and creep strength) to be mobilized at the critical sections. Hence, the collapse load of floating ice sheets under long-time loading can probably be estimated as proposed for ideally plastic plates.

The method of analysis⁴⁴ assumes that the material obeys the Tresca yield condition and the associated flow rule where the shearing strength equals one half the yield strength in tension.

For a large floating ice sheet, cracked radially into numerous long wedges, the total collapse load at the tip is found to be:

$$P_0 = \frac{4\pi M_0}{1 - \frac{a}{2L}} \quad \text{for } 0.2 < \frac{a}{L} < 1. \quad (66)$$

Equation 66 is shown in Figure 31 for various values of a/L . This figure can be used either for ductile failure with the limit plastic moment M_0 under long term loading conditions or for brittle failure with the elastic resisting moment M_b .

Some approaches have been made⁵⁴ to take into account the time-dependent deformation of an ice sheet by making hypotheses as to the rheological behavior of ice. Further information is required however on the creep properties of various ice types before the results can be applied.

Application of analysis. Figure 31 summarizes the results of computations which are pertinent in obtaining the maximum vertical force that ice can exert on an isolated construction. The upper curve was obtained by overestimating the radius of the circle of collapse and is on the safe side so that the maximum force can safely be predicted for the usual range of small structures. The main difficulty in applying these results is, here again, in choosing an acceptable value for the flexural strength of ice. Surveys have been made on the similar question of the collapse loads on floating freshwater ice sheets used as roads, bridges and landings by pulp and paper companies in Canada.^{30 65} The collapse loads varied mainly from about $P = 100 h^2$ to $P = 500 h^2$, where P is in pounds and h in inches. If this is compared with the plastic theory for the highest values and the elastic one for the lowest we find that the flexural strength of ice varies from $\sigma_b = 80$ to 200 psi. This is compatible with results obtained directly from standard flexural tests of river and lake ice.^{28 35}

The case which has been considered up to now is that corresponding to a load distributed over the area of a small circle. The case of a load distributed over the area of a rectangle may be obtained by methods developed for simply-supported plates.⁷⁴ The equivalent of a square area, in particular, is a circle of radius $r = 0.57 a$, a being the length of the side of the square. The effect of any group of concentrated loads on the deflection of the infinitely large plate can be calculated somewhat by summing up the deflections produced by each load separately.⁴⁴

Actually, the reactions are not distributed over the area of the structure but along its periphery. It is thus difficult to derive the stress distribution theoretically. For construction of a rectangular form it may be safe to replace the shape by a form with straight sides and semicircular ends. Then the lifting force on the straight sides can be computed in the same manner as for a long straight wall.

For a group of piles of rectangular overall form, the U.S.S.R. standard recommends that the total uplift force be taken as for a circle of radius $r = \sqrt{ab}$, where a and b are the sides of the rectangle.

Vertical force on a straight wall

This case can be simulated by a strip load acting on an infinite plate on an elastic foundation. If a number of equal, central concentrated loads are applied in line on a floating ice sheet, the analysis is simplified by ignoring longitudinal bending and using an equivalent strip load of $2p$ per unit length (Fig. 30).

The differential equation of the deflection of this long beam is:

$$\frac{d^4 w}{dx^4} = \frac{q - sw}{D} \quad (67)$$

where, as previously, q is the applied load, s the foundation modulus, and D the flexural rigidity of the plate.

In this case of loading, $2p$ per unit length, the solution is:

$$w = \frac{p}{sL} e^{-x/L\sqrt{2}} \sin\left(\frac{x}{L\sqrt{2}} + \frac{\pi}{4}\right) \quad (68)$$

For the elastic state the maximum positive transverse bending moment M_r , per unit length, under the center of the load is:

$$M_r = \frac{pL}{\sqrt{2}} \quad (69)$$

The maximum negative transverse moment occurs at a distance of about $x = 2.2L$ from the load and is, approximately, $M_r = -0.14pL$. The maximum deflection is:

$$w_0 = \frac{p}{sL\sqrt{2}} \quad (70)$$

and the width of the deflection band is about $x = 3.3L$. The yield load at which the first longitudinal crack develops at the bottom of the ice sheet below the load can be estimated from eq 69. A strip load has to be more than $3L$ from the edge of large sheets to satisfy the above equations and develop the estimated yield load.

Chankin¹⁴ has proposed a formula very like eq 69 for computing the maximum force acting on a straight wall. He found this formula to be valid for a variation of water level of from 0.3 to 1 in./hr, ice thickness 3 ft, with a value of E of 60×10^4 psi as obtained from measurements in an artificial reservoir.

In the case of a very rapid rise of water level ΔH , Lofquist¹² proposed to use the same formula when the ice is considered to be an elastic material. We then have:

$$p = sL\Delta H\sqrt{2} \quad (71)$$

where

p = load on the structure, lb/ft

s = foundation modulus, 62.4 lb/ft³

ΔH = water rise, ft

L = radius of relative stiffness, ft.

This gives the unit load directly as a function of the variation in water level. In contrast with the case of the isolated load on an ice sheet, the first failure, directly in contact with the wall, is the final one as the wall cannot transmit any more load to the sheet thereafter. With a value of E of 60×10^4 psi, the deflection w_0 at failure is 2.7 in. for a 1-ft-thick sheet of 200 psi bending strength, and 4.8 in. for a 3-ft-thick sheet. These values of the water level fluctuation can be attained quite rapidly in a river.

The maximum load can also be obtained for the ideal rigid plastic plate. The elastic yield moment of ice M_b should, however, correspond to the full plastic bending moment M_0 . The only difference is the change of M_b by M_0 , and the maximum possible vertical force is given by the same equation (eq 69) which gives here a higher value for p .

$$p = \frac{M_0 \sqrt{2}}{L} \quad (72)$$

Strength of adhesion of ice to structures

In some cases the maximum vertical force that can be transmitted to a structure might be limited by the strength of adhesion of ice to the material the structure is made of. Unfortunately there are very few available data on this basic mechanical property of ice and, as for other properties, there is a lot of scatter in the experimental results because of insufficient control of the uniformity of the structure of the ice and of other relevant factors.

It has been shown⁷⁷ that the adhesive strength of ice is a linear function of the temperature up to a point where it becomes larger than the internal shear or cohesive strength of the ice itself. The sharp transition between the adhesive and the cohesive break occurs at $8\frac{1}{2}^\circ\text{F}$ (-13°C) for strong snow ice between two stainless steel plates.

Among the results of experimentation for artificial ice are those shown in Table IX which were obtained for rather high rates of loading, on the order of 5 psi/sec, and results depend strongly on the rate. It must be noted that in most cases the strength of adhesion of ice to construction materials is as high as the shear strength of the river or lake ice itself, which is usually taken to be from 80 psi to 150 psi.⁷

ICEBREAKERS^{76 77}

Introduction

Icebreakers operate either under arctic conditions or in ice formed in a temperate climate. These conditions are widely different. Arctic ice is usually several years old, several feet thick, solid, and very hard because of the low prevailing temperatures. The ice in the temperate zones is softer as it is only a few months old and usually not more than 3 ft thick. However, it has the tendency to raft and form pack ice of extensive dimensions. In rivers there are often accumulations of frazil and slush ice right down to the bottom of the navigation channel. We shall be more concerned here with this latter type of ice and the operation of icebreakers in navigable rivers and lakes.

Icebreakers are best defined by their primary functions: to break solid ice, to maneuver in heavy concentrations of pack ice, and to clear channels through which other ships can pass in safety. Ice-strengthened ships, in contrast, are normally cargo transport ships strengthened for use in ice. Heavily reinforced hulls, a sloping forefoot and a ratio of horsepower to displacement of more than unity are characteristics common to both types. The icebreaker is usually distinguished by more powerful engines, higher ratio of beam to length, smaller cargo capacity and such distinctive

Table IX. Adhesion of ice to various materials and coatings (Freiberger and Lackner¹⁹).
Rate of load application at 5 psi/sec.

	<u>Ice adhesion, shear (psi)</u>
Metals:	
Mild steel	120
Stainless steel	115
Copper	125
Aluminum	90
Nickel	85
Zinc	90
Galvanized steel	110
Woods:	
Douglas fir	45
Courbaril	65
Lignum vitae	80
Plastics:	
Polymethyl methacrylate	40
Cellulose acetate	25
Glass:	65
Rubber:	20 to 150
Paints:	
Gray deck paint (Navy)	80
Haze gray paint (Navy)	100
Resin films:	
Acrylics	80 to 130
Alkyds	75 to 95
Epoxy's	80 to 130
Polytetrafluoroethylenes	60 to 70
Polytrifluorochloroethylene	90
Phenolics	30 to 110
Silicones	40 to 95
Urethanes	95 to 130
Vinylidenes	50 to 80
Vinyls	90 to 115

features as heeling tanks. Icebreakers designed for use in interior waters, as in the Gulf of St. Lawrence, may possess one or two forward propellers which are not used in polar icebreakers.

The first ships modified for breaking ice were tugs and harbor vessels with reinforced bows and increased power. They cleared ice and assisted the passage of cargo ships in and near harbors. The first icebreaker, in the true sense, was *Eisbrecher 1*, built in Hamburg in 1871 for service on the River Elbe. In 1890 the Finnish *Murtaja* represented the greatest advance in the European type of

icebreaker. It was able to break 20-in.-thick solid ice with no snow cover, but was helpless in ice-slush and snow-covered ice. The full-lined bow pushed the snow and slush forward with the result that the ship was forced to a stop.

At the same time the development of icebreakers on the Great Lakes proceeded along new lines. These vessels, which got into difficulty in pack ice, were able to force their way through by backing into the ice. The natural consequence was that icebreakers were built with bow propellers. Thus in 1888 and 1893 the ferryboats *St. Ignace* and *St. Maria* were built with both stern and bow propellers. The primary action of the bow propeller was to wash water and broken ice away from the forward end of the ship and thus reduce the friction between the ice and the bow. Furthermore, the ship could break into pack ice by alternately running backward and forward on the bow propeller, so that water and the ship were forced into the pack ice. The work of one bow propeller is, however, asymmetrical because of the unbalanced torque reaction and in modern inland icebreakers there are two of them, rotating in opposite directions.

The first polar icebreaker, the Russian *Ermak*, was completed in Newcastle, England, in 1899. With the advance of shipbuilding technology, the design, power and size of icebreakers developed steadily. By the outbreak of World War II, they were in common use in the Baltic, the Gulf of St. Lawrence and, though less frequently, in the Russian and Canadian Arctic. Military demands during the war stimulated the building of the Russian *Stalin* class and the United States *Wind* class icebreakers. Renewed postwar activity has included the building of increasingly large and powerful icebreakers such as the Argentine *General San Martin*, the Canadian *Labrador*, *John A. MacDonald* and *Louis St. Laurent*, the Japanese *Fuji*, and the Russian *Moskva* class. The Russian *Lenin* with a hitherto unprecedented nominal horsepower of 44,000 was the world's first nuclear-powered surface ship. All these ships are primarily polar icebreakers. The development of other icebreakers has similarly been rapid, particularly for use in the Baltic.

The mechanics of icebreaking

There are three different situations, depending upon the character and thickness of the ice, which an icebreaker may have to deal with: the breaking of a continuous ice sheet at a constant speed, the discontinuous ramming of thick strong ice, and finally the movement through nonhomogeneous ice consisting of a mixture of rafted ice and slush. These cases will be dealt with successively.

Icebreaking at constant speed. An icebreaker acts on a solid ice sheet in two ways. As the vessel moves onto the ice it exerts a force in the plane of the ice sheet that crushes the ice in the immediate vicinity of the stem and may produce long radial cracks starting from this point. The forces normal to the ice sheet produce bending which, initially, causes radial cracks to emanate from the center of loading because of tension in the bottommost fibers of the ice sheet. As loading is increased, the radial cracks lengthen and increase in number until finally a circumferential crack, roughly at right angles to the radial cracks, is formed by tension in the uppermost fibers of the ice sheet.

The icebreaking operation is essentially discontinuous and rhythmic. Films taken during experiments with the *Mackinaw*⁶⁴ and other observations show that the ice first cracks in radial directions from the stem and then breaks ahead in directions at right angles to the radial cracks. The broken sectorial pieces turn around on their edges and pass along the icebreaker's side. Since the overall width of these broken floes is less than the icebreaker's beam, the sides of the bow come in contact with the ice sheet and a further two or three rows of floes are produced by bending failure. Some floes are forced under the ice field on the side of the ship but the majority are broken into smaller pieces under the hull and appear behind the ship in the channel it has made. This breaking action is essentially of the vibratory type. When the bow of the vessel moves forward

it is deflected upward over unbroken ice, which is broken up on the downswing. The frequency of the vibrations depends on the length of the broken pieces and the speed of the ship. The amplitude builds up for every cycle until the vibrations get out of phase due to local variations in the thickness and constitution of the ice. This is fortunate, because long-duration resonance vibration could easily lead to fatigue failures in the hull, where the heaviest bending moment occurs. The largest amplitudes measured during the test with the *Mackinaw* were 8 mm ($\frac{5}{16}$ in.).

For the same power, the shape of the bow is the most important factor affecting the efficiency of the icebreaking operation.⁶⁹ Because the flexural strength of ice is normally about half as much as its compressive strength, the general concept, of course, is to have a small bow angle that will increase the vertical load component for the same horizontal one. But there is a limit to the sharpness and inclination of the forefoot. If too much ice is broken by flexural loading, large slabs are forced down along the body and appear at the propeller, where they are liable to impose undesirable shock, or in the wake where they interfere with successful convoy work. If the bow angle is steep and the buttock lines too full, the resistance set up by the broken ice as it passes down and out becomes great, the force required to break the ice in compression is high, and the efficiency is low for the same power. In the latter stages of this operation the ice becomes broken so small that it actually looks like the bow wave of open navigation. In the final instance the bow should be shaped to give acceptable-size floes in the wake with the minimum expenditure of power.

The exact shape of the forebody that will produce such a result in different cases is not known because the force that each type needs to break an ice sheet of given thickness and quality has not been determined. This is so because of the extremely complex conditions of ice loading, the theoretical difficulty involved in the analysis of the stress distribution in the ice sheet, and the little-known behavior of the ice itself at collapse.

A physical model represents the best approach to the solution of that problem in each case if a suitable material can be found to represent the ice. A first and very rough approximation can be obtained from a simplified mathematical model where only the vertical component of the force exerted by the bow is taken into account. The loading is then assumed to be distributed over sectors of a semiinfinite sheet made of individual wedges resting on an elastic foundation and, finally, the collapse is taken to be that of a perfectly elastic body. The analysis⁵⁰ then shows that for a small area of loading on the edge of a semiinfinite sheet made of 45° unit sectors, the vertical force at collapse is approximately:

$$P = 3 M_b \quad (73)$$

where M_b is the maximum yield bending moment of ice per unit width

$$M_b = \frac{\sigma_b h^2}{6} \quad (74)$$

and σ_b is the flexural strength of ice and h its thickness.

Because the force required to break the ice sheet depends essentially on the characteristics of the ice and the form of the bow, this most important resistance that ice is offering to an icebreaker is independent of its speed.

In the icebreaking process, it is recognized that there are two types of ice forces³³ resisting a ship moving in a solid ice sheet: direct ice forces and dynamic forces. The first, which do not depend on the icebreaker's speed, are: resistance to breaking of the ice at the stem and along the sides of the ship, resistance to tilting and submerging of the floes, dry friction of the floes along

the icebreaker's hull, and resistance coming from wave generation during the oscillatory movement of the ship and the floe. The dynamic component is the resistance of water to the floe movement to which must be added the inertia forces which occur when the speed of the pieces of ice is accelerated from zero up to some fraction of the speed of the vessel.

The direct forces depend upon the characteristics of the ice and the dimensions and shape of the icebreaker. The hydrodynamic and inertia forces also depend on the ice dimensions and the form of the ship but principally they depend on the square of the ship's velocity, if the speed is not too low. The following semiempirical formula⁵⁴ has thus been proposed to represent the ice resistance to a moving ship:

$$R = (C_1 + C_2 V^2) Bh, \quad (75)$$

Where R is the ice resistance in pounds, V is the speed in knots, B the beam in feet and h the ice thickness in inches.

The values of C_1 and C_2 are in a way a measure of the efficiency of an icebreaker in a continuous operation although they must still be slightly dependent on h . There are still very few reliable measurements of C_1 and C_2 . They are of the order of 40 and 1.5 for the *Mackinaw*.⁵⁴

Icebreaking by ramming. For very thick ice the icebreaking process is no longer continuous in the forward direction. Instead the icebreaker starts at some distance from the ice and runs into it at maximum speed. As the speed is reduced to zero, kinetic energy is transformed into icebreaking work.

Because all available energy is concentrated on breaking the thick ice sheet by bending only, this case is usually considered to be the critical one in the design of polar icebreakers.³⁶ In contrast to continuous movement, there is no resistance from isolated floes in the channel, and in addition to the engine forces, the inertia of the ship is available to break the ice.

The fundamental analysis of the maximum capability of a ship to break ice by ramming has been developed by Vinogradov.⁶⁶ He assumes that an icebreaker moving at a known velocity strikes a uniform ice sheet. The bow of the ship glides up until the downward pressure reaches a magnitude which causes the ice sheet to collapse as can be estimated roughly using eq 73. He assumes that because of the short time involved the thrust is horizontal at all times and that the geometry of the water plane is not seriously affected.

The principle of conservation of energy is applied. The energy expended is the ship's kinetic energy plus the work done by the propeller thrust acting through the distance traveled. The energy expended is directed into three channels: 1) energy dissipated by impact of the bow of the ship; 2) potential energy due to the ship being raised and changed in trim; 3) frictional loss caused by rubbing of the ship against the edge of the ice. In the case when the ship stops at the instant of ice collapse:

$$E_1 + E_2 = E_3 + E_4 + E_5 \quad (76)$$

where:

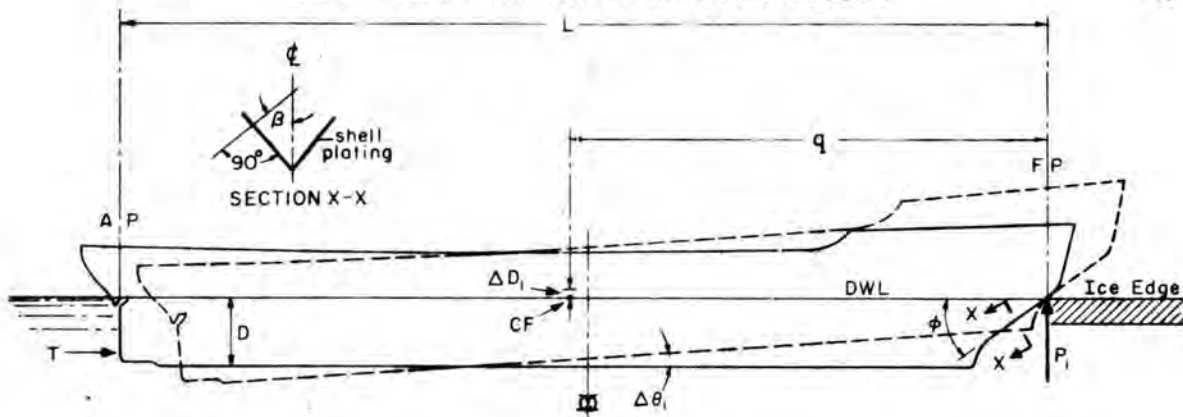
E_1 = kinetic energy of the ship when the ice is first touched

E_2 = energy derived from propeller thrust

E_3 = energy dissipated by impact

E_4 = potential energy acquired by the ship

E_5 = energy loss by friction.



- | | | | |
|----------|---|------------------|---|
| L | Length between perpendiculars | CF | Center of flotation = center of water plane area |
| B | Beam at water line | M_L | Longitudinal metacenter, the point about which the ship pitches |
| D | Draft, loaded | m_L | Longitudinal metacentric height = GM_L (measures stability) |
| V | Submerged volume | P_1 | Maximum value of vertical reaction at stem |
| S | Draft water plane area | T | Propeller thrust |
| W | Displacement = loaded weight | ϕ | Angle of stem with horizontal |
| a | Water plane area coefficient = S/LB | $\Delta\theta_1$ | Maximum angular change of trim |
| δ | Block coefficient = V/LBD | ΔD_1 | Maximum change in draft at CF |
| G | Ship's center of gravity | | |
| CB | Center of buoyancy = center of submerged volume | | |

Figure 32. Variables and nomenclature used in ramming analysis.

Let W represent the weight or displacement of the ship and V_0 the velocity of the ship when the ice is first touched. Kinetic energy absorbed during the operation (assuming negligible speed after impact) is:

$$E_1 = \frac{W}{2g} V_0^2. \quad (77)$$

The next item considered is the energy delivered by the propellers to the ship while it is gliding up on the ice edge. During this interval there is a reduction in mean draft designated by ΔD_1 and the ship assumes an angle of trim of $\Delta\theta_1$ (Fig. 32). The distance from the point of contact of the stem to the center of flotation is designated by q . The stem of the ship is sloped at angle ϕ from horizontal. Then from the instant of first contact until the ice collapses, the linear advance of the ship is:

$$\Delta D_1 \cot \psi + q \Delta\theta_1 \cot \psi.$$

Let T represent the average value of propeller thrust during this advance; then

$$E_2 = T(\Delta D_1 + q \Delta\theta_1) \cot \psi \quad (78)$$

This formula should be expressed in different terms so as to include P_1 , the maximum value of the vertical force developed at the stem. Assuming that P_1 is small compared with the displace-

ment W , and that the change in draft and trim do not seriously change the properties of the water plane, we then have $\Delta D_1 = P_1/w_1 S$, S being the water plane area and w_1 the density of sea water. The angle of trim $\Delta \theta_1$ depends on the applied moment $P_1 q$ and the longitudinal metacentric height m : thus $\Delta \theta_1 = P_1 q/Wm$. This energy term can then be expressed as:

$$E_2 = T \left[\frac{P_1}{w_1 S} + \frac{P_1 q^2}{Wm} \right] \cot \psi.$$

The water plane area S equals the product of length, beam and water plane area coefficient, $S = LBa$. The weight of the ship equals the product of length, beam, draft, block coefficient and density of sea water, or $W = LBD\delta w_1$. New nondimensional coefficients k_1 and k_2 are arbitrarily set up by relationships $q = k_1(L/2)$ and $m = (k_2^2 a^2 L^2)/D\delta$. Substituting these new quantities in the last equation, we get:

$$E_2 = A \frac{DP_1}{W} T \cot \psi \quad (79)$$

where

$$A = \frac{\delta}{a} \left[1 + \left(\frac{k_1}{k_2} \right)^2 \frac{1}{4a} \right].$$

According to the theory of impact, when two bodies collide normally there is always a dissipation of energy, whose magnitude depends on the relative velocity and a physical constant e known as the coefficient of restitution. Now the stem of the ship does not collide normally with the edge of the ice. The component of initial velocity V_0 which is directed normal to the edge of the ice is $V_0 \sin \psi$ and the energy dissipated by impact should be:

$$E_3 = \frac{W}{2g} (V_0 \sin \psi)^2 (1 - e^2). \quad (80)$$

The author does not believe that there is such a type of elastic impact as given by Vinogradov and this term should instead take into account the crushing of an ice wedge in the ice shelf corresponding to the horizontal force developed during the process.

$$E_3 = \int \sigma_1 A_n dn = \frac{\sigma_1 y^3 \tan \psi}{3} \tan \alpha \quad (81)$$

where σ_1 is the indentation strength of ice, A_n the area of contact between hull and ice and dn the distance element normal to the shell through which the force moves. If the ice deformation is small the linear advance of the ship corresponds to the length of the crushed wedge of ice:

$$y = \Delta D_1 \cot \psi + q \Delta \theta_1 \cot \psi$$

and from previous considerations:

$$E_3 = \sigma_0 \frac{A^3 D^3 P_1^3}{3 W^3} \cot^2 \psi \tan \alpha. \quad (82)$$

The vertical force P is a variable which keeps increasing as the ship slides up on the ice. The total rise of the point on the stem at which P is first applied equals the reduction in draft ΔD_1 plus the angle of trim, in radians, times the horizontal arm between the center of flotation and the stem $\Delta \theta_1 q$. The potential energy set up by the force P is therefore

$$E_4 = \int_0^{\Delta D_1} P d \Delta D + \int_0^{\Delta \theta_1} P q d \Delta \theta. \quad (83)$$

Energy is dissipated by sliding friction between the shell plating and the ice. The coefficient of sliding friction f must be applied to that component of the pressure which is normal to the plating. The resultant frictional force F acts in a direction parallel to the stem of the ship and is a variable; half of it acts on one side of the stem and half on the other.

The energy dissipated by frictional force F acting through a distance determined by the changes in draft and trim is given by:

$$E_5 = \frac{1}{\sin \psi} \int_0^{\Delta D_1} F d \Delta D + \frac{1}{\sin \psi} \int_0^{\Delta \theta_1} F q d \Delta \theta. \quad (84)$$

Consider an inclined plane intersecting the bow of the ship in a direction normal to the stem. This section of the bow appears as a wedge with essentially flat sides and the normal pressure on these sides makes an angle β with the centerline plane. As the bow rides up on the ice shelf it forms a wedgelike groove. Pressure is developed normal to the faces of the groove, and friction along the faces of the groove directed parallel to the sloping stem.

Let R be the resultant force acting normal to the stem. On each side, then, the force acting normal to the plating is:

$$\left(\frac{R}{2}\right)\left(\frac{1}{\cos \beta}\right).$$

So the frictional force is given by

$$F = f R \left(\frac{1}{\cos \beta}\right) \quad (85)$$

The magnitude of the force R is related to other forces acting on the ship as follows:

$$R = P \cos \psi + T \sin \psi.$$

Equation 83 can be rewritten as:

$$E_4 = \int_0^{\Delta D_1} \left[P \frac{\cos \psi}{\cos \beta} + T \frac{\sin \psi}{\cos \beta} \right] d \Delta D + \int_0^{\Delta \theta_1} \left[P q \frac{\cos \psi}{\cos \beta} + T q \frac{\sin \psi}{\cos \beta} \right] d \Delta \theta. \quad (86)$$

Using eq 84 in eq 82, combining with eq 81 and substituting the previously established values, $P = w_1 S \Delta D$, $Pq = W m \Delta \theta$, and others, we get:

$$E_4 + E_5 = \frac{AD}{W} \left[\left(1 + f \frac{\cot \psi}{\cos \beta} \right) \frac{P_1^2}{2} + f \frac{TP_1}{\cos \beta} \right]. \quad (87)$$

Substituting all the values of component energies in eq 83 there finally results:

$$A \left[\left(\frac{P_1}{W} \right)^2 - 2X \frac{P_1}{W} \frac{T}{W} \right] = Y \frac{V_0^2 [1 - (1 - e^2) \sin^2 \psi]}{gD} \quad (88)$$

in which:

$$X = \frac{1 - \left[\frac{f}{\cos \beta} \right] \tan \psi}{1 + \left[\frac{f}{\cos \beta} \right] \cot \psi} \cot \psi$$

$$Y = \frac{1}{1 + \left[\frac{f}{\cos \beta} \right] \cot \psi}$$

From eq 76 we obtain the downward icebreaking force P_1 as given by Vinogradov:

$$P_1 = XT + \left\{ X^2 T^2 + \frac{YW^2 V^2}{AgD} [1 - (1 - e^2) \sin^2 \psi] \right\}^{\frac{1}{2}} \quad (89)$$

Taking the actual energy of crushing the ice instead of the theoretical energy of elastic impact (eq 82) we get:

$$P_1 = \left\{ -\frac{b}{2} + \left(\frac{b^2}{4} + \frac{a^3}{27} \right)^{\frac{1}{2}} \right\}^{\frac{1}{3}} + \left\{ -\frac{b}{2} - \left(\frac{b^2}{4} + \frac{a^3}{27} \right)^{\frac{1}{2}} \right\}^{\frac{1}{3}} - \frac{S}{3} \quad (90)$$

where

$$S = \frac{3W^2}{2\sigma_0 A^2 D^2 Y \cot^2 \psi \tan \beta}$$

$$a = -2XTS - \frac{S^2}{2}$$

$$b = \frac{2}{27} S^3 + \frac{2}{3} XTS^2 - \frac{YW^2 V^2 S}{ADg}$$

The values of the coefficients X and Y depend on the dynamic friction of ice on the metal surface which is usually taken as 0.10 to 0.15 for fresh and brackish water ice and 0.20 for salt water and polar ice.³⁶ One of the important factors involved is the presence of a snow cover on the ice shelf that greatly increases the coefficient of dynamic friction and reduces the efficiency of the icebreaking operation. The parameters T , W , V_0 , D and A are characteristics of the ship and are discussed at length by Milano.⁴⁷

Icebreaker operations in pack ice. Accumulations of ice floes, snow, slush, brash and frazil ice, usually called pack ice in the sea, and ice dams in rivers, often produce the greatest difficulties for an icebreaker. It is not possible to skirt the heaviest positions as the ice conditions underneath the surface are usually unpredictable.

It is in pack ice that the bow propellers of icebreakers are exceptionally useful. They produce water lubrication between the bow of the vessel and the ice. Furthermore, they break the ice into smaller pieces and the wake of the icebreaker becomes clearer. There is also a possibility of working on the ice by running in reverse on the bow machinery, while during the forward motion of the stern propeller the water will be thrown forward. The bow propellers should be inward rotating so that the wash of the bow is more powerful and effective on both sides of the vessel. Observations have shown that the heaviest mass of water is then thrown against the bow at approximately a quarter of the length from the stem. The stern propellers, however, should be outward rotating so as to throw the ice pieces outwards and give a clearer track.

Another advantage of two bow propellers is the better maneuverability they give the vessel. At low speed and in heavy ice the action of the rudder is weak, but by suitable regulation of revolutions and the direction of rotation of the propellers, one can make the vessel move at will, even directly sideways. But the bow-propeller system has drawbacks. The costs are higher than with stern propellers only and the water and ice resistance are higher. The total propulsion efficiency is also smaller for the same power. For polar operation where thick hard ice is encountered, icebreakers are not designed with bow propellers because of the decrease in ramming ability.

In heavily rafted light field-ice, heavy slush, and frazil ice, the action of ramming of an icebreaker is not really efficient because the ice just packs closer and forms a stronger cushion after each successive charge. One practice on the St. Lawrence River¹⁰ has been to use the propellers as drills to dislodge the ice pieces from the accumulation. This action is slow but positive and sometimes takes place under conditions where the ice jam is so high that parts of it fall on the deck. A ship with two forward propellers is then quite an asset. Otherwise the ship proceeds astern with its stern propellers acting as drills. All Canadian icebreakers^{69 76} are fitted with underwater gear which will stand up to the impact of breaking ice astern and propellers which will in effect drill drift ice piled as high as 20 to 30 ft.

When a ship is moving entirely in an unconsolidated ice cover or pack ice, covering part or all of the water surface, no energy is required to break the solid sheet, but the friction of the ice on the ship's hull increases considerably. This additional friction force can be expressed by a formula similar to the one used to determine the drag resistance of a ship in water only:⁵³

$$R = C_d \frac{\rho S V^2}{2} \quad (91)$$

where R is the ice resistance in pounds, V the ship's speed in feet per second, S the wetted surface of the hull in square feet and ρ the density of water. Figures 33 and 34 give some data on the value of R for icebreakers of the U.S.S.R. For ice concentrations of almost 100% of the surface area an empirical formula has been proposed by Buzuev and Ryblin based on measurements on the *Stalin* and *Kapitan Belousov*:¹⁰

$$R = 8.6 L^{0.25} B^{0.25} (0.4 + 8.0 N_{Fr}^{1.25}) \quad (92)$$

where R is the ice resistance in metric tons, L and B the ship length and beam in meters and N_{Fr} the Froude number of the ship V/\sqrt{gL} .

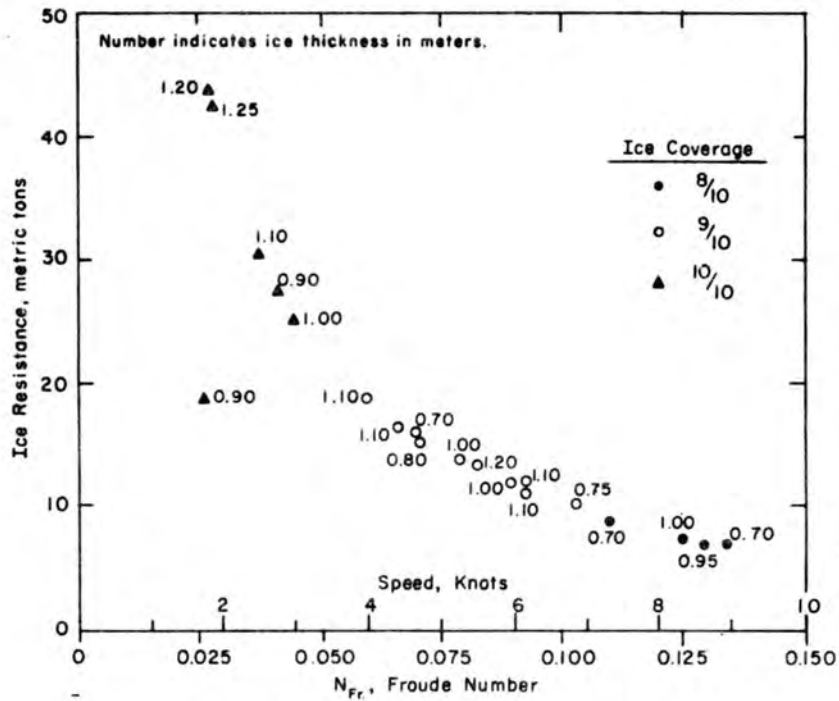


Figure 33. Ice resistance in pack ice of Lena.¹⁰

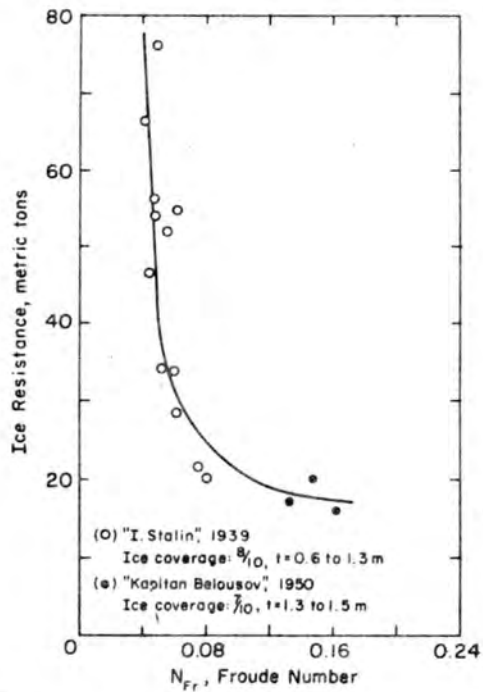


Figure 34. Ice resistance in pack ice for the Stalin and Kapitan Belousov.¹⁰

The resistance of ice pieces accumulated in ice ridges, heavily rafted ice or frazil and slush ice dams is unknown at present.

Characteristics of Icebreakers

The normal task of an icebreaker is to assist other vessels through the ice. Other tasks include the destruction of river ice jams to prevent flooding (Fig. 35), winter ferry services, supply of isolated arctic harbors, patrol, buoy tending and hydrographic surveying.

When assisting vessels in smooth waters the icebreaker makes an open track and the other vessels follow as closely as possible without risking collisions. At sea and in rivers this is often difficult because the track does not stay open because of currents and wind. One or more of the vessels may get stuck in the ice. To cut it loose the icebreaker must approach closely. Here good maneuverability is of great importance. The ideal is to have two icebreakers, with the wider of the two opening the way while the other offers loosening services if required, as done on the St. Lawrence River. In very difficult conditions it may even be necessary for the icebreaker to tow the ship it is assisting.

The characteristics of some recent icebreakers are shown in Table X. The most important main dimension of the icebreaker is its beam, which determines the breadth of the vessel it is capable of assisting. The track that the icebreaker leaves is about 2 ft wider than the ship itself. With regard to length, the important points are that a short vessel has good maneuverability, while a longer one has more room for machinery and engine power and can therefore break through heavier ice. For the majority of icebreakers of the oceangoing variety the usual practice has been to adopt a water line length/water line beam ratio in the range of 4.0 to 4.5. It is believed⁷⁶ that there is an opportunity for improvement in polar operations by increasing the length/beam ratio to the range of 5.0 to 5.5.

If there are no restrictions on draft due to water depth, the draft should be large enough to accommodate large propellers placed as low as possible so as not to draw down air. As the stern propellers are usually designed for higher power and lower revolutions than the bow propellers, their diameter is larger. This difference is overcome by designing the icebreaker for a 2-ft trim aft which also makes it easier to reverse out of ice walls. The large trim and tank capacities on icebreakers make it possible, within certain limits, to alter the draft and the trim of the vessel.

The typical proportions and lines of an icebreaker (the U.S.S. *Glacier*) are shown in Figure 36. The upper portion of the stem is nearly vertical. At water line and below, the stem slopes close to 30° and there is a final step in its lower portion to prevent the ship from riding too far on the ice edge and getting stuck. The midship sectional shape is close to a circular arc with a center above the water line. The virtue of the circular section appears to be that it facilitates working the ship loose by means of the heeling tanks when beset. The first effect of the heeling moment is to break the grip of the static friction and this is followed by a loosening of the ice adjacent to the hull. This shape tends to make the block coefficient very small, somewhat lower than 0.5 for typical icebreakers. It produces very little damping to any induced rolling motion and icebreakers are heavy rollers in the open sea if stabilizing fins are not fitted. The after-body form of an icebreaker usually narrows to a point, and a generous clearance is provided between propeller blades and shell so as not to let any ice lodge in between.

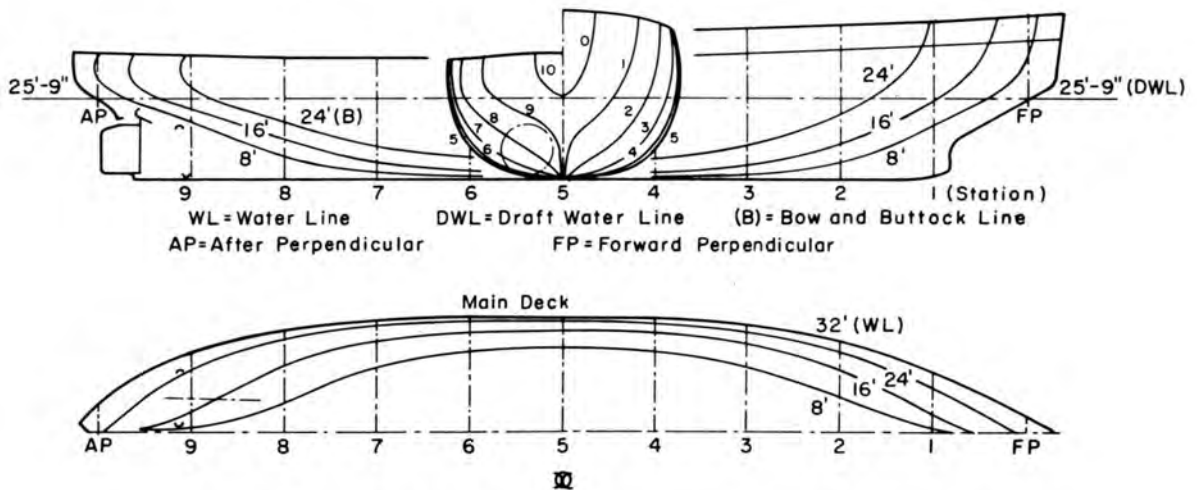
All modern icebreakers have heeling tanks that can be put to use in one or two minutes. By pumping water from one side to the other a heel of 5 to 8° to either side can be achieved, which is normally sufficient to loosen the vessel from the ice. The capacity of ballast tanks in icebreakers is high and may reach 15% of the displacement. In certain cases the icebreaking efficiency can be increased by pumping water between trim tanks in the fore and aft peaks, thus changing the trim.

Table X. Icebreakers without fore propellers. (Compiled from various sources.)

1 Vessel	<i>Murtaja - Ermak</i>	<i>Stalin</i> class	<i>Kirov</i> class	<i>d'Iberville</i>	<i>General</i> <i>S. Martin</i>	<i>Labrador</i>	<i>Glacier</i>	<i>Moskva</i> class	<i>Lenin</i>	<i>John A. MacDonald</i>	
2 Year of delivery	1890	1899	1937-39	1938-40	1953	1954	1954	1955	1959	1960	
3 Shipyard	Bergsunds	Armstrong	Leningrad Nikolajev	Leningrad	Lauzon	Weser	Sorel	Ingalls	Wartsila	Leningrad	Lauzon, Quebec
4 Nation	Finland	U.S.S.R.	U.S.S.R.	U.S.S.R.	Canada	Argentina	Canada	U.S.A.	U.S.S.R.	U.S.S.R.	Canada
5 Region of operation	Abo	U.S.S.R.	Arctic Ocean	Far East	Arctic Region	Antarctic	Arctic Region	Antarctic	Arctic Ocean	Arctic Ocean	Arctic Ocean
6 L oa (m)	47.5	97.5	106.0	109.0	94.5	84.7	82.0	94.5	122.1	134	96
7 L wl (m)	41.9	94.6	102.1	101.0	92.0	76.95	76.2	90.0	112.4	128	93.5
8 B max (m)	10.98	21.64	23.16	22.3	20.27	19.00	19.35	22.56	24.50	27.6	21.4
9 B wl (m)	10.77	21.42	22.70	21.2	19.66	18.60	18.90	22.0	23.50	27.5	21.0
10 Draft, normal (m)	4.75	7.32	8.00	7.25	8.38	6.50	7.85	8.53	9.50	9.2	
11 Draft, max (m)	5.51	8.54	9.04	8.4			8.86		10.50		8.9
12 Moulded depth (m)	7.60	12.95	12.61		12.20	9.85/7.50	11.51		14.00/11.50	16.1	
13 Displacement normal metr. tons	825	7875	9300	8330	8840		5350	8763	13100	16000	
14 Displacement max. metr. tons	900	10000	11000	10250			6580		15200		8150
15 Normal total power HP (metric)	1200	7500	10050		10800	7500	10500		26000	44000	12000
16 Max. total power HP (metric)	1793	9000		12000	15200	8100	12000	24000			
17 Main machinery normal power HP (metric)						2×3750	6×1750		8×3250		
18 Main machinery max. power HP (metric)				4×3000		2×4050	6×2000	10×2400			
19 Main machinery rot. speed R.P.M.				300		275/300	810	720/810	330		
20 Stern propeller m/c normal power HP (metric)	1×1200	3×2500	3×3350		2×5400	2×3250		2×8450	2×5500 1×11000		
21 Stern propeller m/c normal power HP (metric)	1×1793	3×3000		2×2600 1×5200	2×7600	2×3550	2×5000	2×10500			3×
22 Stern propeller rot. speed R.P.M.	83	105	105		145	138	145	120/175	105/120	185/205	
23 Type of machinery	Steam	Steam	Steam	Diesel el.	Skinner st.	Diesel el.	Diesel el.	Diesel el.	Diesel el.	Atomic-steam turbine	Diesel el.
24 Normal/Max. speed knots	—/12.5	14/—	—/15.5	—/—	15/—	—/16	16/—	18/19(?)	18/19.5	15.5/18	—/19.5



Figure 35. The John A. MacDonald breaking a jam at the Quebec bridge over the St. Lawrence River, 1968.



Draft D: 25 ft 9 in.	Block coefficient: 0.48
Displacement at DWL: 7400 tons	(Displaced volume/LBD)
Length on DWL, L: 290 ft 0 in.	Midship-section coefficient: 0.77
Beam on DWL, B: 72 ft 6 in.	Freeboard amidships: 12 ft 7 in.
L/B ratio: 4.00	

Figure 36. Lines and particulars of U.S.S. Glacier.

Special methods are sometimes used to assist in the icebreaking process. One consists of spraying warm water from the circulating pumps onto the ice at the stem. Explosives, salt melting and even manual ice cutting may be used in exceptional circumstances. Large bow vibrators have been used in small river icebreakers in the U.S.S.R. A recent ice ferry has the capability of ejecting warm compressed air from deeply submerged outlets in the forebody.

The technique of icebreaking in Arctic waters consists to a large extent of searching out a way through leads in the ice where resistance is least. Since the view from the mast is comparatively limited several arctic icebreakers carry one or two helicopters which can take off from the aft deck for reconnaissance.

ICE MODELS

Introduction

In the last few years knowledge of the mechanical behavior of ice has increased to the point where some basic laws can be formulated and scaled down for physical models to study engineering problems caused by ice. The first such models were built just after World War II in Canada,²⁶ with paraffin to model the ice, and in the U.S.S.R.,⁶⁴ with weakened ice and paraffin.

The technique of ice modeling has evolved along two completely different lines. On one side studies were made on moving ice in rivers and the similitude was limited to representing the hydrodynamic conditions, the ice itself being considered a rigid, unbreakable body. On the other side, models were built to measure the forces caused by the impact of ice on structures, particularly on icebreakers, and the similitude was aimed mainly at scaling down the strength properties of ice, somewhat neglecting other dynamic aspects.

Laws of complete similitude

The laws of similitude of an ice model can be obtained by extending the standard methods of hydraulics.⁶¹ A hydraulic or mechanical model is said to be in complete similitude if it has geometric, kinematic, and dynamic similitude. The model is geometrically similar if the distances between corresponding points of the model and the prototype are in the same ratio for all points in the model. This can be expressed as:

$$l = \lambda l_m \quad (93)$$

Where l and l_m are the distances in the prototype and the model respectively and λ is the geometric scale.

The model is kinematically similar if, at corresponding geometric points and corresponding times, velocities and accelerations are in constant ratios. Thus

$$v = v_* v_m \quad (94)$$

$$a = a_* a_m \quad (95)$$

where v , v_m are prototype and model velocities; a , a_m are prototype and model accelerations; and v_* , a_* are the velocity and acceleration scale ratios. It thus comes directly from previous relations that the time scale t_* should be related to other scales by:

$$\lambda = v_* t_* \quad (96)$$

$$\lambda = a_* t_*^2 \quad (97)$$

Finally a model is dynamically similar if at all geometrically equivalent points, for corresponding times, the forces in the model and the prototype appear in a constant ratio:

$$F = F_* F_m \quad (98)$$

where F , F_m are the prototype and model forces and F_* is the force scale. This last condition is sufficient to determine all other scales of the model. If all the forces appear in the same ratio F_* for corresponding places and-times, it is clear that the equations of mechanical equilibrium will be the same everywhere in the model and the prototype. All terms of the equations for the model will differ by the product of the same constant from the equation of the prototype. This constant would be F_* for the equations of equilibrium of forces and λF_* for work and energy equations. Model and prototype having the same equations will thus behave in exactly the same dynamical manner.

This last condition leads to a simple method for obtaining all other scale values. It is only necessary to express each of the forces that has to be taken into account in the ice model and to keep the same force ratio F_* for each of them. This will be done in the more general case of complete similitude of an ice model.

Forces of gravity on water, ice and structures in water. The force of gravity can be expressed by:

$$F = \rho g l^3 \quad (99)$$

where ρ is the density of the materials with subscripts 1, 2, 3, . . . ; g is the acceleration of gravity; and l is a characteristic length of the material.

As it is not feasible to change g on a model,

$$F_* = \rho_* \lambda^3 \quad (100)$$

$$\rho_* = \rho_{1*} = \rho_{2*} = \rho_{3*} \dots$$

If water is used on the model it then follows that all other substances should have the same density that they have in the prototype:

$$\rho_* = \rho_{1*} = \rho_{2*} = \rho_{3*} = 1.$$

So that eq 100 then becomes:

$$F_* = \lambda^3 \quad (101)$$

which is the basic expression of the force scale.

Forces of inertia of water, ice and other bodies in water. The inertial force corresponding to any change in velocity in water, ice and other bodies as, for example, waves, current changes, slowing down icebreakers, etc., can be expressed as:

$$F = \rho l^3 \frac{dv}{dt} \quad (102)$$

where dv/dt is the total acceleration of the representative mass. This gives:

$$F_* = \frac{\lambda^3 v_*}{l_*}$$

and with eq 96:

$$F_* = \lambda^2 v_*^2.$$

Comparing with eq 101:

$$v_* = \sqrt{\lambda} \quad (103)$$

which corresponds to the Froude similitude where the Froude number $N_{Fr} = V/\sqrt{gl}$ is kept the same on model and prototype. It can be easily seen that the Froude similitude comes out by comparing only the force of inertia with the force of gravity. If there is any acceleration whatsoever in an ice model it has to be scaled down with the Froude similitude.

Forces of water friction. The water friction forces on different boundaries, including ice, can be represented by:

$$T = C \left(\frac{\epsilon}{l}, N_{Re} \right) \rho \frac{V^2 l^2}{2} \quad (104)$$

where T is the tangential friction force, C is the friction coefficient depending on relative roughness ϵ/l and Reynolds number N_{Re} , V is a representative velocity outside the boundary layer and l^2 is the surface on which T is acting.

For rough turbulent flow, as is most generally found in natural rivers, the friction coefficient is independent of the Reynolds number. To get the same coefficient on the model and the same quadratic law it is necessary to have complete roughness similarity and a Reynolds number high enough to ensure rough turbulent flow at the reduced scale. For river models there is thus a limitation in the choice of the scale that should be big enough to obtain this acceptable Reynolds number.

When a body is towed in water the friction force also has the same form as eq 104 and becomes independent of N_{Re} if the velocity is high enough. The friction force in the developing laminar boundary layer then becomes small before that of the fully developed turbulent layer and the same reasoning applies as for the previous case. In all cases the conditions of similitude from eq 104 are:

$$F_* = \lambda^2 V_*^2$$

which gives exactly the same as eq 103:

$$v_* = \sqrt{\lambda}.$$

The friction force is also in complete Froude similitude if the Reynolds number is high enough on the model.

Forces of water pressure. The forces of water pressure, which are always normal to a surface, can be expressed by:

$$N = p l^2 \quad (105)$$

where p is the water pressure and l^2 is the representative surface. In similitude this gives:

$$F_* = p_* \lambda^2$$

which, with eq 101, gives the pressure scale ratio:

$$p_* = \lambda. \quad (106)$$

The ratio of inertia forces to pressure forces corresponds to the well known Euler number.

Ice friction forces. The friction of ice on other ice or on foreign substances can be expressed by:

$$T = f N \quad (107)$$

where T and N are the tangential and normal forces and f is the static or dynamic friction factor. It can readily be seen, from similitude of the forces, that the friction factor has to be the same in the model as in the prototype.

Internal ice forces at collapse of an ice sheet. If brittle failure of a floating ice sheet of thickness h is considered for the prototype and the model and if also in both cases the failure can be predicted from elastic theory, three types of forces have to be taken into account corresponding to possible modes of failure:

Shear failure forces:

$$T = \tau_0 h l C_1 \left(\frac{a}{l}, \frac{b}{l}, \frac{c}{l}, \nu \right) \quad (108)$$

Crushing failure forces:

$$N = \sigma_0 h l C_2 \left(\frac{a}{l}, \frac{b}{l}, \frac{c}{l}, \nu \right) \quad (109)$$

Flexural failure forces:

$$P = \sigma_b h^2 C_3 \left(\frac{a}{L}, \frac{b}{L}, \frac{c}{L}, \nu \right) \quad (110)$$

where T , N and P are the forces producing failure; τ_0 , σ_0 and σ_b are the shear, compressive and flexural strength of ice; l , a , b , and c are representative lengths (the last three for conditions of loading); ν is Poisson's ratio; and L is a characteristic length of the ice sheet that is related to the position of the line of collapse:

$$L = \sqrt[4]{\frac{E h^3}{12 \rho g (1 - \nu^2)}} \quad (111)$$

Comparing these relations with the basic force similitude given in eq 101 we then get:

$$\tau_{0*} = \sigma_{0*} = \sigma_{b*} = \lambda \quad (112)$$

and

$$L_* = \lambda \text{ or } E_* = \lambda(1 - \nu)_*^2. \quad (113)$$

Scales for complete similitude. The complete similitude of an ice model, taking into account the previous forces, is thus the Froude similitude. Using water as a material in the model, the following scales have to be taken:

Geometric scale	$\lambda = l_m/l$
Velocity scale	$v_* = \sqrt{\lambda}$
Acceleration scale	$a_* = 1$
Time scale	$t_* = \sqrt{\lambda}$
Force scale	$F_* = \lambda^3$
Mass scale	$m_* = \lambda^3$
Pressure scale	$p_* = \lambda$

The model ice sheet should then have the following characteristics:

Thickness scale	$h_* = \lambda$
Strength scales	$\tau_{0*} = \lambda$
	$\sigma_{0*} = \lambda$
	$\sigma_{b*} = \lambda$
Young's modulus scale	$E_* = \lambda$
Poisson's ratio	} same in model and prototype.
Friction factors	

The surface characteristics of all solid material represented in the model should be the same, to scale, as for the prototype.

Other negligible forces in nature are surface tension forces. Care should be taken that they do not play a role in the model and in particular the model ice should get wet as the real ice does. In the same order of ideas, the model should be big enough to ensure turbulent flow as in the prototype.

Practical limitations to ice modeling

The first difficulty in trying to make an ice model arises from the extreme variability of the properties of the natural ice to be represented. Ice moving down a river may vary in form from frazil particles a few millimeters in diameter, agglomerating together to form very loose flocs, to solid ice pans many feet in length, width and thickness that will pack closely together in a jam. At the same place in a river, there might be no drifting ice during one winter (all ice forming and melting in place) and the maximum amount the upstream stretch can ever produce the following winter. An icebreaker may progress in a solid continuous ice sheet but most often it will go through extremely variable conditions of hummocked ice, following leads going through brash ice, ridges, etc. In the same way, the strength properties of ice vary within wide limits even for the same type of ice and even from hour to hour for the same piece of ice if temperature and radiation conditions keep changing.

Thus it is impossible to design an ice model that would reproduce all these natural conditions at the same time. Because only one type of ice will normally be represented by the model some design values for the ice properties have to be fixed at the start to be representative of the conditions to be studied. At times extreme values will be taken, as, for example, in choosing high values of ice strength for icebreaker design. At other times, average properties can be chosen, as for the size of the model ice floes to represent conditions of frazil, slush or ice jams at break-up.

The main difficulty in trying to make an ice model is to find a suitable material to model ice at a reasonable scale. Up to now four materials have been used for ice modeling: polyethylene, wood, paraffin and ice. Polyethylene and wood are used in small pieces to represent drifting ice floes. The density, roughness and average form of the drifting ice can be reproduced but it is impossible to break the ice pieces in the model, so none of its internal properties are modeled. Weakened ice is produced by freezing brine very quickly with a method developed by the Arctic and Antarctic Institute of the U.S.S.R. The fine-sized ice crystals thus produced have a flexural strength of the order of 5 psi, which would make for a scale of $\frac{1}{40}$ if compared with 200-psi strong ice in bending. The modulus of elasticity and the shear and compressive strengths are not then to the same scale, which makes for a distortion in the results that is hard to appreciate. Furthermore, it is a considerable undertaking to operate a big model under cold room controlled conditions. Paraffin and model-making wax have been used to study the internal behavior of an ice sheet. These materials are very strong, with a flexural strength on the order of 150 psi, so that theoretically the similitude is practically impossible at an acceptable scale. In some recent models, additives have been put in the wax, such as soap powder, coal dust and kerosine, considerably reducing the strength of the model ice. Such methods have led recently to suitable materials to model ice at an appropriate scale.⁷⁶

Models representing only the hydrodynamic behavior of ice

In hydrodynamic models the conditions of internal collapse of the continuous ice sheet are not represented. The ice is essentially made of individual unbreakable pieces whose hydrodynamic behavior is simulated. The Froude similitude applies well and the only difficulty in choosing model ice is to represent the dimensions, forms and surface friction effects of the floes.

One of the very first studies made to simulate such an effect was carried on in a ship-towing tank to obtain the resistance of an icebreaker in brash ice of various surface concentrations.⁵³ The model ice was paraffin-molded in hexagonal pieces and tests were made at various scales to determine the coefficient of ice resistance as shown in Figure 37. It can be seen that scales ranging from $\frac{1}{40}$ to $\frac{1}{100}$ seem to be adequate for that purpose if the Froude number is higher than 0.15.

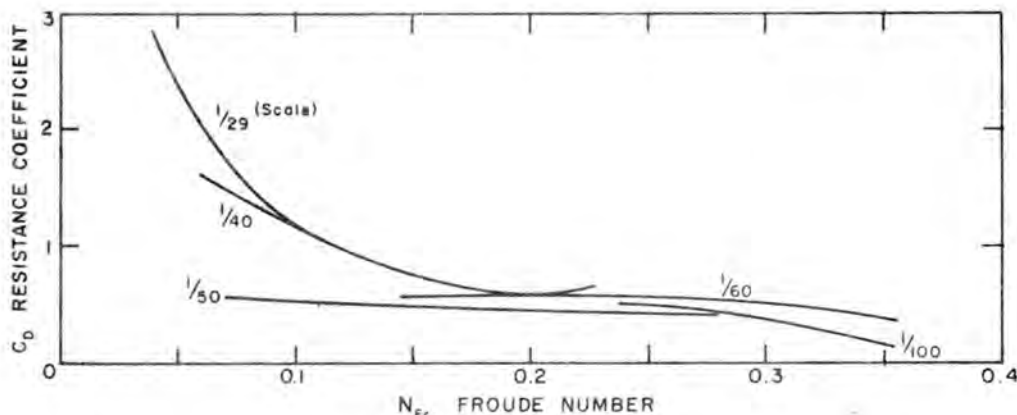


Figure 37. Coefficient of resistance in ice ($\frac{1}{10}$ covered) for scale models of icebreaker Lenin.

A big ice model was built to represent a stretch of more than 5 miles of the St. Lawrence River at scales of $\frac{1}{240}$ horizontally and $\frac{1}{130}$ vertically.⁷⁹ The aim of the study was to determine the effect on ice jams in Montreal Harbour if new land were reclaimed for Expo 67. This site was known to be subject to frazil and slush ice jams up to about 30 ft in depth with water level rises approximately 20 to 25 ft above summer levels. The frazil floes, slush and floes were represented on the model by small polyethylene grains whose surfaces were treated to get a wetting effect and increase the roughness. The model was built according to standard hydraulic laboratory procedures for fixed bed models and the bed roughness was adjusted for clear water conditions. The model was then fed with ice by automatic feeders whose rates were simulated according to computed values in nature. The ice runs were then made on the model, simulating natural conditions, and the results of water level measurements on the model and in the prototype are shown in Figure 38. In nature the jams form during cold weather and there is always some bonding by thermal exchanges between ice floes at the water surface. On the model there is no cohesion at all between the ice pieces, and the pack is much less resistant to thrust and shoves than in nature. The ice accumulations are thus bigger on the model, the head losses increase and the water levels are higher. The model thus errs on the safe side and gives the worst limiting conditions.

Another example is a model built to study the flow of frazil ice on a river in Iceland.¹¹ An intake to a power plant had to be designed that would get water free of ice while the heavy frazil ice run would be disposed of at the top of a regulating weir. Polyethylene foam of very small size was used with success to represent the heavy balls of aggregated particles of frazil.

Ice models are most useful to study floods caused by ice during the spring breakup of rivers. For those conditions there is practically no thermal influence during the relatively short period of jam formation, and model results may be expected to give a good approximation of the truth. Figure 39 shows such a model in operation where a temporary ice-delaying structure made of a boom and a control weir had to be studied. Conditions of ice accumulation and dry jam formation were studied in the model. Model ice consisted of $\frac{1}{4}$ -in.-thick by 1-in.-square polyethylene blocks, surface treated, which simulated the average characteristics of the ice floes at breakup for this site at a scale of $\frac{1}{120}$. One of the difficult aspects in this type of study is the representation of the solid ice sheet being broken up and pushed back under the thrust of the unconsolidated ice accumulation. On this model the problem was quite local and the solid sheet in the pond formed by the weir was just simulated by a floating wooden boom. This boom was first placed at the upstream end of the pond. When the accumulation became unstable and was shoved under the boom it was moved

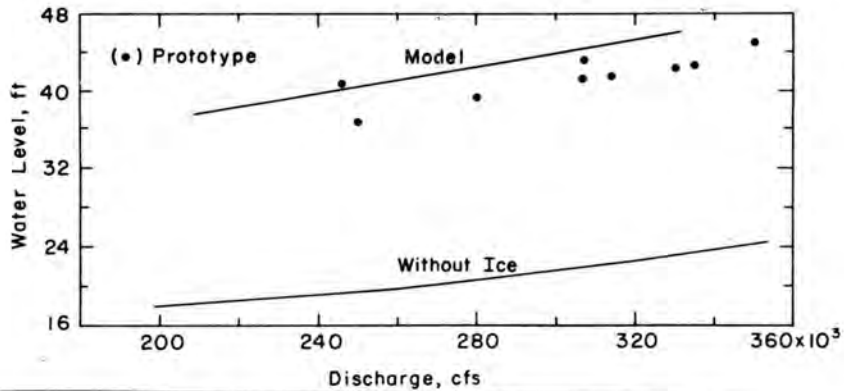


Figure 38. Water level and discharge for model and prototype.



Figure 39. Model of an ice-retaining boom, Laval University (1967).

artificially down, by trial and error, to a new section where the pack ice was again stable. The final retaining place was, of course, the position of the designed structures at the top of the weir. This process is indeed quite crude and there is no doubt that there is a lot of room for improvement in the techniques of ice model studies of this type.

Models for studying the collapse of an ice sheet

Models in which a solid ice sheet has to be broken have been used up to now practically only for the design of icebreakers and bridge piers. The technique is very young and even the basic laws of similitude are being questioned.⁷¹

The main difficulty here is to use a material that would simulate all properties of ice at suitable scales, such as those normally used in model ship towing tanks. If a too-strong model

material is used, such as untreated paraffin or more or less normal ice, a distortion has to be introduced to various scales of ice properties in order to interpret the results.⁵² A distortion could also be introduced only in the scale of the model ice thickness. If this scale is given by

$$h_m = h_* h \quad (114)$$

the distortion factor D is

$$D = \frac{\lambda}{h_*} \quad (115)$$

It can readily be seen from eq 99, 102, 104, and 105 that the forces of gravity and inertia on the ice of the model are distorted by a factor D but that the friction and pressure forces on ice are correctly scaled down.

For certain problems, like the ramming of an icebreaker to a stop on a solid ice sheet where there is no ice movement until failure, the external forces of gravity and inertia of the ice shelf need not be taken into account and a distortion is possible in the thickness scale of the ice. The only conditions of similitude left are, then, the similitude of crushing, sliding up of the ship, and final bending collapse of the sheet. Starting with the most important one (eq 110) concerning the final collapse we get

$$F_* = \sigma_{0*} h_*^2 \quad (116)$$

Choosing

$$L_* = \lambda \quad (117)$$

in order to get a conservation in horizontal length for collapse of the sheet so that all geometrical properties of the ship stem would be at the same scale in plan relative to failure cracks.

The crushing and shearing forces are also reproduced with eq 108 and 109:

$$F_* = \tau_{0*} \lambda h_* = \sigma_{c*} \lambda^2 \quad (118)$$

so that the final scale ratios required for simulation of the ice sheet in that case would be:

Geometrical	λ
Thickness	$h_* = \lambda/D$
Strength	$\tau_{0*} = D\lambda$
	$\sigma_{0*} = D\lambda$
	$\sigma_{b*} = D^2\lambda$
Young's modulus	$E_* = D^3\lambda(1 - \nu_*)^2$

Because in the total energy budget for this process the energy required for crushing and shearing the ice is usually very small, these aspects may be left out in the actual simulation. With the model material properties σ_{bm} and E_m , it is then possible to fix the scale values λ and D for each application.

For other phenomena like the continuous movement of an icebreaker in an ice field, or the impact of a floe on a pier, the ice pieces are quickly accelerated or decelerated and the inertia of the ice cannot be neglected. In a primary analysis no particular element of the energy budget seems negligible and complete similitude is normally required. It must, however, be realized that no model ice will reproduce simultaneously all the properties of real ice. The geometry of secondary failure might be quite different with model ice because of the usual nonisotropic behavior of real ice and its weakness in shear along vertical planes. The size of the small broken-up pieces in a model may thus be distorted, changing the overall friction effects, as for an icebreaker.

Future of ice modeling

There are very few mechanical problems brought up by ice that are amenable to an appropriate solution by mathematical computations only, because of always-complex boundary conditions. Such is the case of a river section where the flow of water and ice combine to fix the water profile. Such is the case of the loading characteristics of an ice sheet rammed by an icebreaker or of a bridge struck by a moving ice jam. In most of these cases, physical models are the most valuable tools for getting acceptable answers to the questions being raised. A better knowledge of basic ice properties combined with the improvement of materials used to simulate ice in models will certainly lead to a great breakthrough in the application of engineering science for the fight against river ice and its use for beneficial purposes.

LITERATURE CITED

1. American Association of State Highway Officials (1957) *Standard specifications for highway bridges*. Section 1.2.17, p. 20.
2. Assur, A. (1962) Discussion on bearing capacity of floating ice sheets. *Transactions of the American Society of Civil Engineers*, vol. 127, part 1.
3. Barnes, H. T. (1928) *Ice engineering*. Montreal: Renouf Publishing Co., 364 p.
4. Brown, E.; Clarke, G. C. (1932) Ice thrust in connection with hydro-electric plant design. *Engineering Journal*, p. 18-25.
5. Buckley (1900) Ice ramparts. *Wisconsin Academy of Science Transactions*, vol. 13, p. 141-162.
6. Bullinger, W. (1955) *Engineering economy*. New York: McGraw-Hill.
7. Butkovich, T. R. (1954) Ultimate strength of ice. U.S. Army Snow Ice and Permafrost Research Establishment (USA SIPRE) Research Paper 11.
8. _____ (1957) Thermal expansion of ice. *Journal of Applied Physics*, vol. 30, no. 3, p. 350-353.
9. _____ (1958) Recommended standards for small-scale ice strength tests. USA SIPRE Technical Report 57.
10. Buzuev, A. and Ryblin, A. (1961) Calculation of the resistance encountered by an icebreaker on moving through ice cakes and brash. *Morskoi Flot*, vol. 21, no. 8, p. 136-138.
11. Carstens, T. (1968) Hydraulics of river ice. *La Houille Blanche*, vol. 8, p. 271-284.

LITERATURE CITED (Cont'd)

12. Carter, D. (1968) Preliminary analysis of controlled formation and of some mechanical properties of columnar ice with horizontal c-axis. (In French.) M. Sc. Thesis, Laval University.
13. Chafir, I.N. and Ginsberg, R.I. (1942) Damage caused to marine works. In ref. 40.
14. Chankin, P.A. (1961) On the stability of concrete revetments on slopes submitted to ice forces. *Cidrotekhnicheskoe Stroitel'stvo*, no. 3.
15. Columbia University Press (1950) Tables of Bessel functions $Y_{0(z)}$ and $Y_{1(z)}$ for complex arguments.
16. Committee of Power Division (1931) Ice as affecting power plants. *Transactions of the American Society of Civil Engineers*, vol. 95, p. 1134-1150.
17. Cook, H.J. (1941) Protecting a reservoir against ice. *Waterworks and Sewerage*, Dec., p. 549.
18. Dorsey, N.E. (1940) *Properties of ordinary water substance*. New York: Reinhold.
19. Drouin, M. (1968) Static ice force on extended structures. N.R.C. Conference on Ice Pressure, Tech. Memorandum No. 92, p. 95-108.
20. _____ (1970) Static ice force on structures. (In French.) D. Sc. Thesis, Laval University.
21. Eckhard, G.F. (1920) Large highway bridge wrecked by pressure of cake ice. *Engineering News*, vol. 84, p. 902-904.
22. *Engineering Record* (1899) Failure of a Minneapolis dam by ice pressure. Vol. 39, p. 542-543.
23. *Engineering News* (1912) Failure of dam from ice pressure. Vol. 65, p. 681.
24. *Engineering News Record* (1967) Pier measures ice pressure. Dec. 14, p. 34.
25. Flinn, A.E. (1928) Arch dam investigations - Ice pressures. *Proceedings ASCE*, vol. 54, no. 3, p. 268-269.
26. Foundation Engineering Co. of Canada (1949) Model study of the Bromptonville ice jam.
27. Frankenstein, G.E. (1959) Strength data on lake ice. USA SIPRE Technical Report 59.
28. _____ (1961) Strength data on lake ice. USA SIPRE Technical Report 80, 6 p.
- Freiberger, A. and Lacks, H. (1961) Ice-phobic coatings for deicing naval vessels. In *Proceedings of The Fifth Navy Sciences Symposium*, p. 234-237.
30. Gold, L.W. (1959) Discussion on *Recent studies on ice - Their application to logging operations in Eastern Canada*. (C.R. Silversides). Woodlands Section, Pulp and Paper Assn., Publication no. 1845, B-1.
31. _____ (1965) The initial creep of columnar-grained ice. National Research Council, Canada, Research Paper 261.
32. _____, Black, L.D., Trofimenkof, F. and Matz, D. (1958) Deflection of plates on elastic foundation. *Trans. Engrg. Inst.*, Canada, vol. 2, p. 123.
33. Hertz, H. (1884) Über das Gleichgewicht schwimmender elastischer Platten. *Wiedemann's Annalen der Physik und Chemie*, Leipzig, vol. 22, p. 449.
34. Hill, H.M. (1935) Field measurements of ice pressure at Hastings Lock and Dam. *Military Engineer*, vol. 27, p. 119-122.
35. Hitch, R.D. (1959) Flexural strength of clear lake ice. USA SIPRE Technical Report 65.
36. Jansson, J.E. (1956) Icebreakers and their design. *European Shipbuilding*, vol. 5.

LITERATURE CITED (Cont'd)

37. Jellinek, H.H.G. (1957) Adhesive properties of ice. USA SIPRE Research Report 38.
38. Kirkham, I.E. (1927) Five Missouri River highway bridges. *Engineering News Record*, vol. 99, no. 19.
39. Komarovskiy, A.N. (1932) The effect of ice cover on hydro-electric installations and means to combat it. Ch. 1 and 12, Energoizdat-Moscow-Leningrad.
40. Korzhavin, K.N. (1962) Action of ice on engineering structures. Novosibirsk, Akad. Nauk. SSSR, 202 p.
41. Krausz, A.S. (1968) Plastic deformation of fresh-water ice. National Research Council, Technical Memorandum No. 92, p. 5-13.
42. Lofquist, B. (1944) Lifting force and bearing capacity of an ice sheet. *Teknisk Tidskrift* No. 25, Stockholm. National Research Council of Canada, Technical Translation 164, 1951.
43. _____ (1954) Studies of the effect of temperature variation - Ice pressure against dams. *Transactions ASCE*, Paper 2656.
44. Meyerhof, G.G. (1962) Bearing capacity of floating ice sheets. *Transactions of the American Society of Civil Engineering*, vol. 127, part 1, no. 3327, p. 524-557.
45. Michel, B. (1967) Ride-up of ice hitting a bridge pier. (In French.) In *Proceedings, XII Congress International Association for Hydrology Research*, vol. 4, p. 279-282.
46. _____ and Drouin, M. (1965) Impact of an ice floe on an obstacle. (In French.) In *Proceedings International Association for Hydrology Research*, vol. 5, p. 60-63.
47. Milano, V.R. (1960) Notes on the preliminary design of icebreakers. M. Sc. Thesis - Webb Institute of Naval Architecture.
48. Monfore, G.E. (1952) Ice pressure against dams: experimental investigations by the Bureau of Reclamation. *Proceedings ASCE*, vol. 78, Technical Separate No. 162.
49. _____ and Taylor, F.W. (1949) The problem of an expanding ice sheet. In *Proceedings of the Western Snow Conference*, 18th Meeting, p. 30-46.
50. Nevel, D.E. (1961) The narrow, free infinite wedge on an elastic foundation. USA SIPRE Research Report 79. AD 277538.
51. _____ (1966) Time-dependent deflection of a floating ice sheet. U.S. Army Cold Regions Research and Engineering Laboratory (USA CRREL) Research Report 196. AD 638717.
52. _____ (1967) Icebreaker simulation. Final report for U.S. Coast Guard by USA CRREL.
53. Nogid, L.M. (1959) Model representation of a ship going through a continuous ice field or pack ice. *Transactions of the Leningrad Shipbuilding Institute*, no. 45.
54. Ormondroyd, J. (1950) Investigation of structural stresses in ice-breaking vessels. Engineering Research Institute, University of Michigan, Project M 720-6.
55. Pariset, E. and Gagnon, A. (1966) Formation of ice covers and ice jams in rivers. *Journal of the Hydraulic Div. Proc. A.S.C.E.*, vol. Hy 6, p. 1-24.
56. Petrunichev, N.N. (1954) Dynamics of ice pressure on hydraulic structures. In *Ledotermicheskie voprosy v Gidroenergetike*. Ed. by D.N. Bibikov, Moscow: Gosudarstvennoe Energeticheskoe Izdatel'stvo, p. 17-46.
57. Pounder, E.R. (1965) *Physics of ice*. New York: Pergamon Press, 151 p.
58. Pratley, P.L. (1938) Collapse of Falls View bridge. *Engineering Journal*, vol. 21, no. 8, p. 375-381.

LITERATURE CITED (Cont'd)

59. Roads and Bridges - News of the month (1945) Ice pressure on Bow River damages bridges. Vol. 83, no. 4, p. 86.
60. Rose, E. (1947) Thrust exerted by expanding ice sheet. *Transactions of the American Society of Civil Engineers*, vol. 112, p. 871-900.
61. Rouse, H. (1955) *Engineering hydraulics*. New York: McGraw-Hill.
62. Schleicher, F. (1926) *Kreisplatten auf elastischer Unterlage*. Berlin: Springer.
63. Shenehan, F.C. and others (1931) Ice as affecting power plants. Final reports of committee of power division, *Transactions of the American Society of Civil Engineers*, vol. 95, p. 1134-1150.
64. Shvayshteyn, Z.I. (1957) Laboratory for studying ice and testing models of icebreakers and ice-strengthened vessels. *Problemy Arktiki*, No. 2.
65. Silversides, C.R. and Rose, L.B. (1958) The preparation of ice landing by pulp and paper companies in Eastern Canada. *Transactions of the Engineering Institute of Canada*, vol. 2, p. 101.
66. Taylor, F.W. (1945) Temperature changes in an ice sheet with the lower surface in contact with water at freezing temperature for various conditions of exposure on upper surface. Memorandum to R.E. Glover, Nov. 29, Bureau of Reclamation, Denver, Colorado.
67. Telechev, V.I., Pinigrin, M.I. and Tolokno, V.V. (1961) Flow of ice through Mamakavskoi hydroelectric works. *Hydraulic Constructions*, No. 7.
68. Vinogradov, I.V. (1946) Ships for navigation in ice. *Oborovgiz NKAP*, 239 p.
69. Watson, A. (1959) The design and building of icebreakers. *Transactions of the Institute of Marine Engineering*, vol. 71, no. 2, p. 37-65.
70. Westergaard, H.M. (1926) Stresses in concrete pavements computed by theoretical analysis. *Public Roads*, vol. 7, p. 25, and New formulas for stresses in concrete pavements of airfields. *Transactions of the American Society of Civil Engineers*, vol. 113, 1948, p. 425.
71. White, R.M. and Vance, C.P. (1967) Icebreakers model tests. *Naval Engineers Journal*.
72. Willmot, J.G. (1952) Measurement of ice thrust on dams. *Ontario Hydro Research News*, no. 3, p. 23-25.
73. Wilson, J.T., Zumberge, J.H. and Marshall, E.W. (1954) A study of ice on an inland lake. USA SIPRE Report 5.
74. Woinowsky-Krieger, S. (1953) Über die Biegung von Platten durch Einzellasten mit rechteckiger Aufstandsfläche. *Ingenieur-Archiv*, vol. 21, p. 331-338.
75. Zlyev, B.V. (1950) Action of ice on lateral booms. *Transactions Moskovskogo Instituta Inzhenerov Zheleznodorozhnogo Transporta*, vol. 74, p. 334-356.
76. _____ (1960) *Transactions of the Society of Naval Architects and Marine Engineers*, vol. 67, 1959. Seven papers on icebreakers, with discussions.
 - a. Ferris, L.W. The proportion and form of icebreakers.
 - b. German, J.G. Design and construction of icebreakers.
 - c. Matthews, F.W. Stability and control of HMCS *Labrador*.
 - d. Lank, S.W. and Oakley, O.H. Application of nuclear power to icebreakers.
 - e. Alexandrov, A.P. et al. The atomic icebreaker *Lenin*.
 - f. Watson, A. Operation of Department of Transport icebreakers in Canada.
 - g. Thiele, E.H. Technical aspects of icebreaker operation.
77. Kashtelian, V.I., Pozniak, I.I. and Ryvlin, A.Ia. (1968) Soprotivlenie l'da dvizheni u sudra (Resistance of ice to the motion of a ship). 2 vol. Sudostroenie, Leningrad.

LITERATURE CITED (Cont'd)

78. Michel, B. (1969) New technique of total simulation of floating ice. *L'Ingénieur*, no. 248, p. 16-20.
79. Hausser, R. (1964) Hydraulic studies for enlarging Notre-Dame and St. Helen Islands. *L'Ingénieur*, June, p. 44-50.

Unclassified

Security Classification

DOCUMENT CONTROL DATA - R & D

(Security classification of title, body of abstract and indexing annotation must be entered when the overall report is classified)

1. ORIGINATING ACTIVITY (Corporate author) U. S. Army Cold Regions Research and Engineering Laboratory Hanover, New Hampshire 03755		2a. REPORT SECURITY CLASSIFICATION Unclassified	
		2b. GROUP	
3. REPORT TITLE ICE PRESSURE ON ENGINEERING STRUCTURES			
4. DESCRIPTIVE NOTES (Type of report and inclusive dates) Monograph			
5. AUTHOR(S) (First name, middle initial, last name) Bernard Michel			
6. REPORT DATE June 1970		7a. TOTAL NO. OF PAGES 79	7b. NO. OF REFS 79
8a. CONTRACT OR GRANT NO.		9a. ORIGINATOR'S REPORT NUMBER(S) Monograph III - B1b	
b. PROJECT NO.		9b. OTHER REPORT NO(S) (Any other numbers that may be assigned this report)	
c. DA Project IT062112A130			
d.			
10. DISTRIBUTION STATEMENT This document has been approved for public release and sale; its distribution is unlimited.			
11. SUPPLEMENTARY NOTES		12. SPONSORING MILITARY ACTIVITY U. S. Army Cold Regions Research and Engineering Laboratory Hanover, New Hampshire 03755	
13. ABSTRACT This monograph summarizes existing knowledge on forces exerted by an expanding ice sheet, impact forces of ice on structures, and vertical forces exerted by ice on hydraulic structures. Sections are also devoted to icebreakers and ice models.			
14. Key Words Ice Icebreakers Model Basins Hydraulic structures Ice breakup			

DD FORM 1473
NOV 66

REPLACES DD FORM 1473, 1 JAN 64, WHICH IS OBSOLETE FOR ARMY USE.

Unclassified

Security Classification